On the way to

Planar Optronic Systems

presented by:

Prof. Dr.-Ing. Ludger Overmeyer

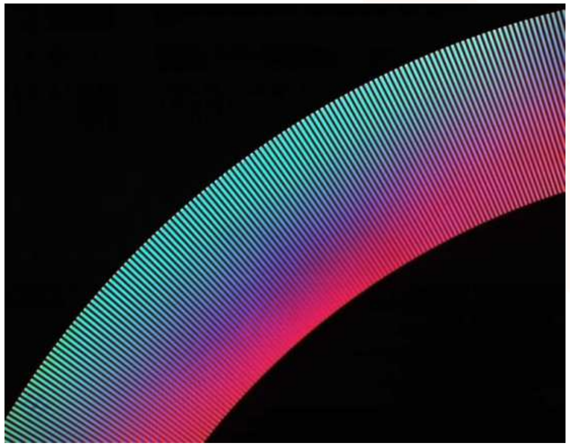

SysInt 2014, Thursday July 3, 2014, in Bremen, Germany

Acknowledgements

The PlanOS science team (alphabetical order)

Meriem Akin	Thomas Hanemann	Welm Pätzold	Laszlo Sajti
Florian Bär	Meike Hofmann	Ann Britt Petermann	Wolfgang Schade
Konrad Bethmann	Christian Kelb	Elke Pichler	Thomas Schmidt
Tobias Birr	Ann-Katrin Kniggendorf	Oswald Prucker	Anne-Katrin Schuler
Patrick Bollgrün	Michael Köhring	Torsten Rabe	Andreas Schwenke
Kort Bremer	Martin Körner	Maik Rahlves	Stanislav Shermann
Boris Chichkov	Jan Gerrit Korvink	Holger Reinecke	Yixiao Wang
Ayhan Demircan	Wolfgang Kowalsky	Carsten Reinhardt	Nan Wang
Sebastian Dikty	Dario Mager	Eduard Reithmeier	Ulrike Willer
Sebastian Döhring	Uwe Morgner	Maher Rezem	Tim Wolfer
Henrik Ehlers	Claas Müller	Lutz Rissing	Merve Wollweber
Ludmila Eisner	Gregor Osterwinter	Detlef Ristau	Marc Wurz
Melanie Gauch	Torsten Otto	Bernhard Roth	Yanfen Xiao
Uwe Gleißner	Ludger Overmeyer	Raimund Rother	Hans Zappe
Axel Günther	Malwina Pajestka	Jürgen Rühe	Urs Zywietz

Funded by **German Research Foundation** (Deutsche Forschungsgemeinschaft)

Outline

- Introduction
- Vision of sensor concepts
- Materials
- Production methods
- Characterization
- Summary

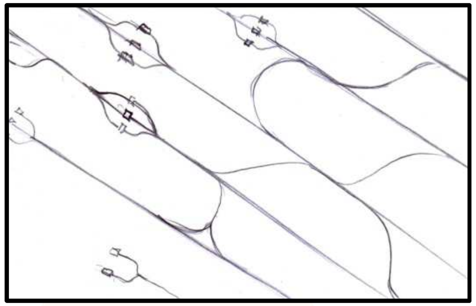

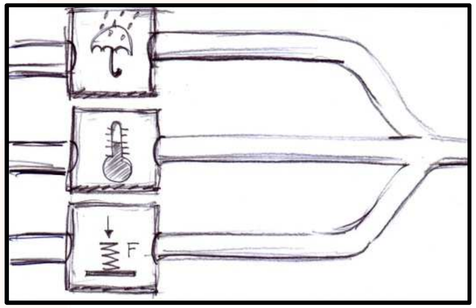

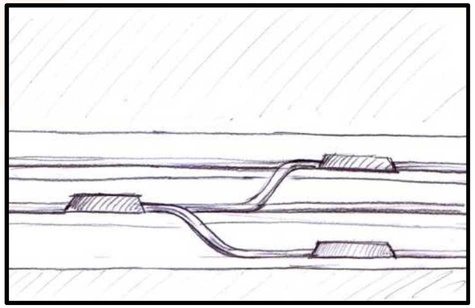

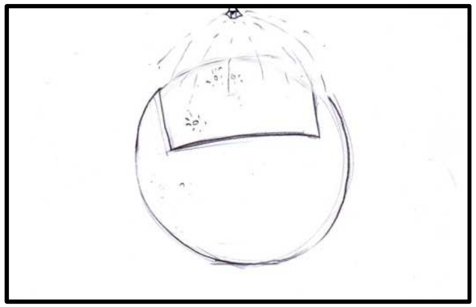

Hypotheses

- Light will be the main future media for signal transmission.
- Measured signals will be converted into light.
- Electrical signals will be exchanged for light signals.
- A fully optical world?
- What do we need to get there?

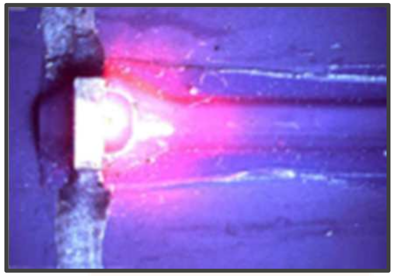

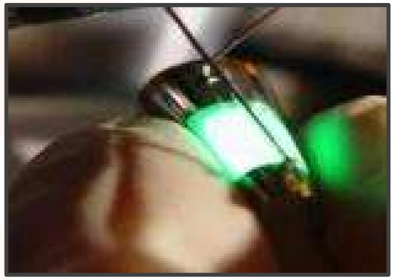
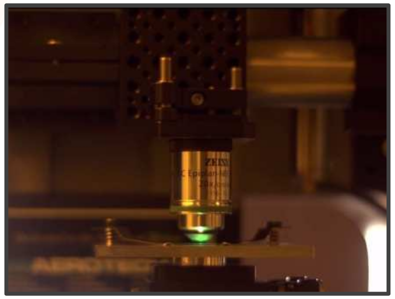

Why optical technologies?

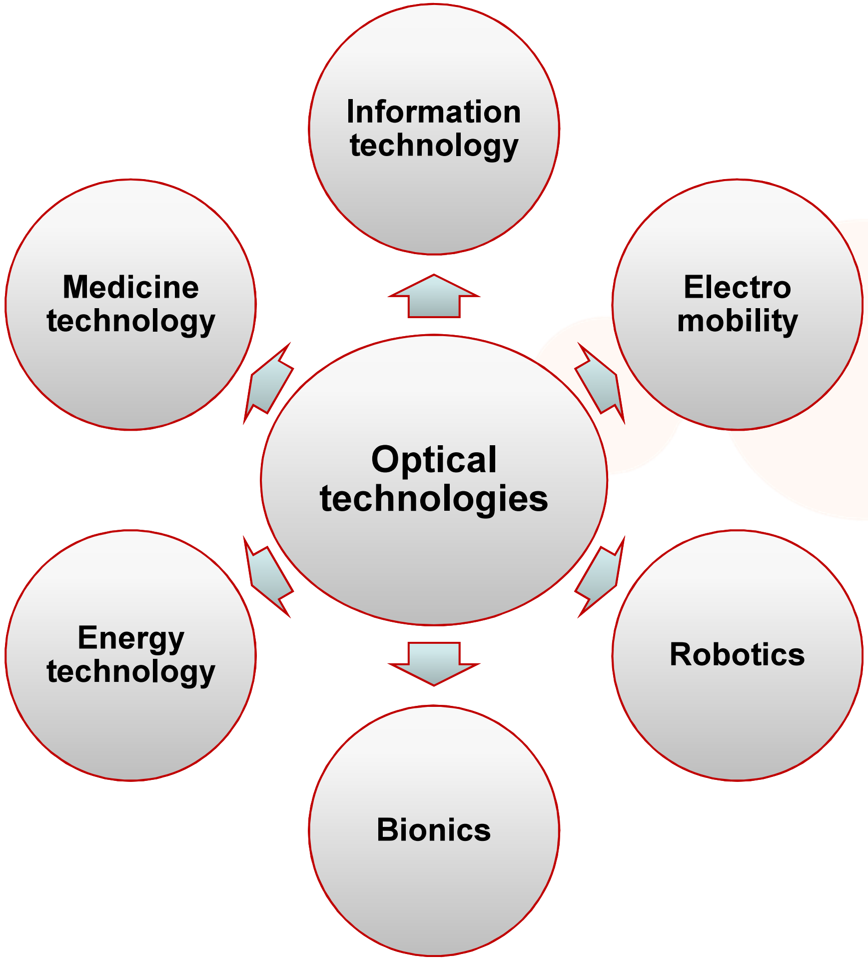

Energy Mobility Environment

Health Communication Security

Assumption:
Optical systems will supplement/replace electronic systems in many areas of application.

Why using photons?

- Variety of planar sensor concepts
- Low energy consumption
- High bandwidth
- Electro-magnetic compatibility
- Simple multiplexing
- High integration density on various scales

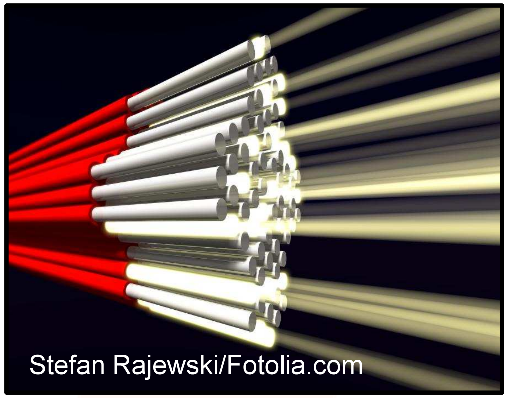

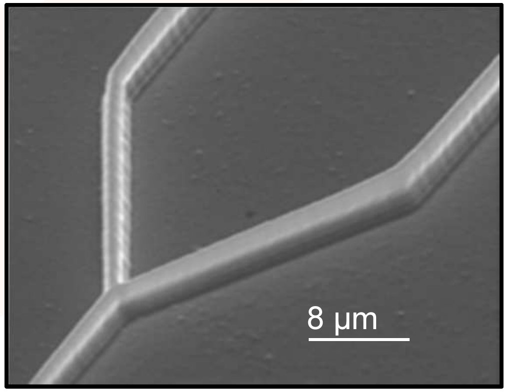

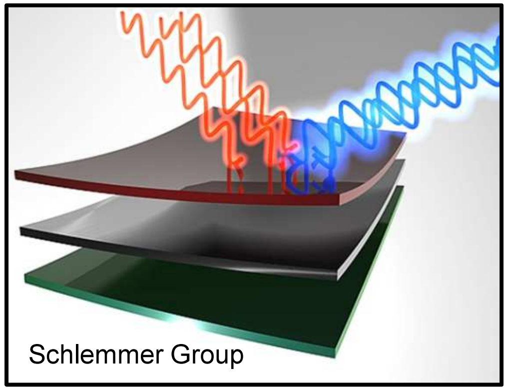

Why planar?

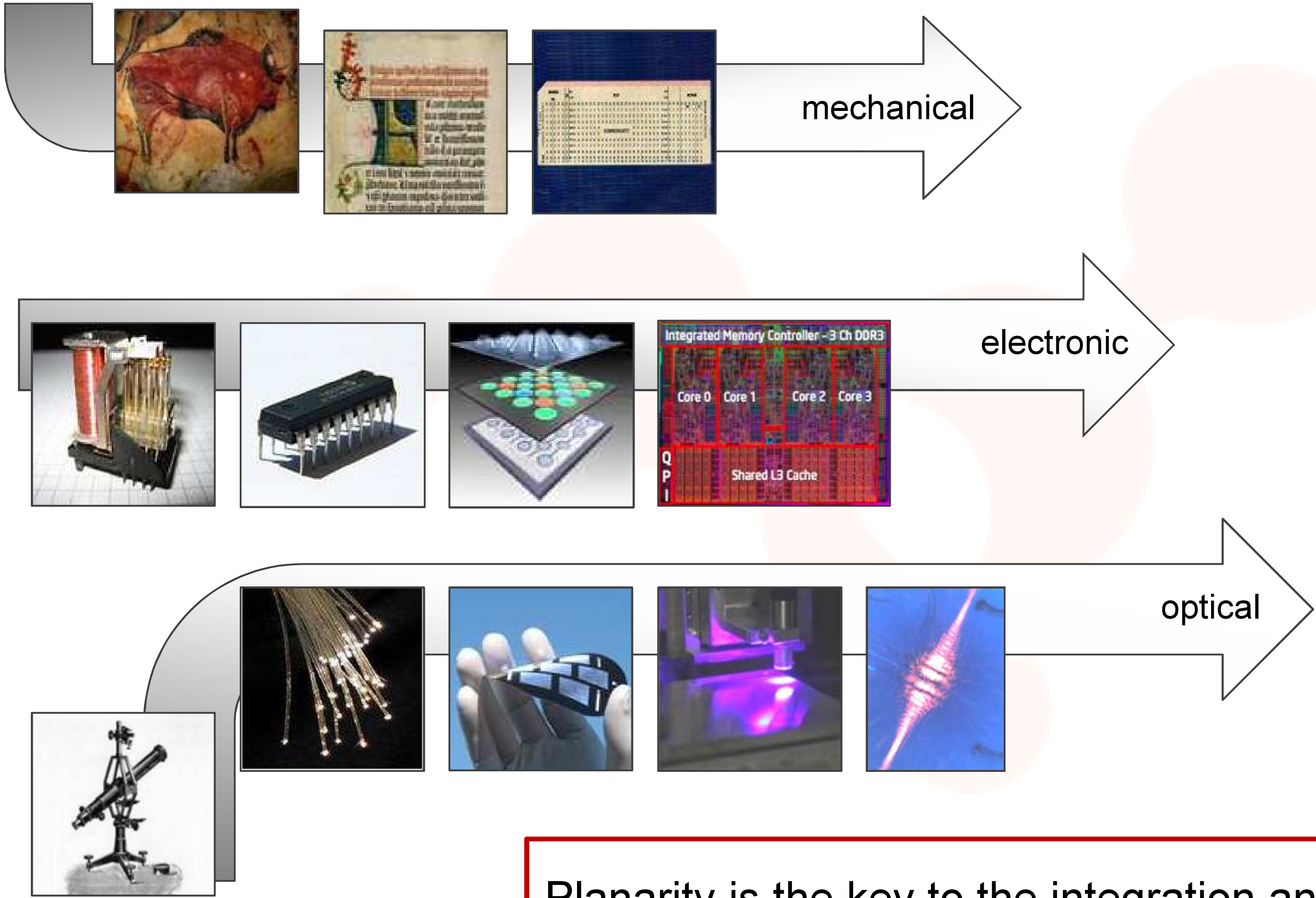

Planarity is the key to the integration and processability in parallel processes.

Why using polymers?

- High functionality; versatile material class
- Modifiable to the application
- Efficient processability, even at high throughput, e.g. reel-to-reel process
- Simple build-up of large-scale systems
- Small layer thickness = high resource efficiency
- Hybrid-systems for trans-technology matrix structures possible

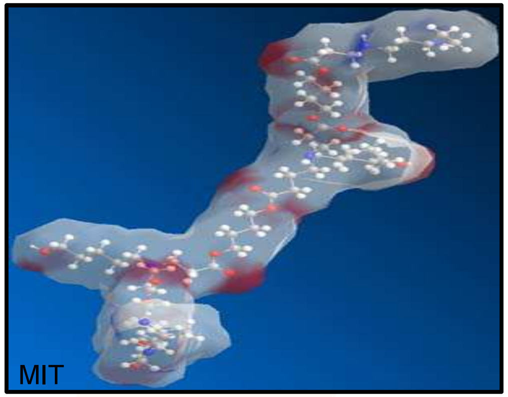

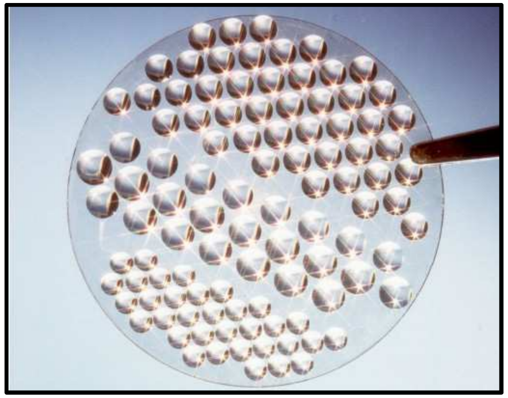

Integration of electronics

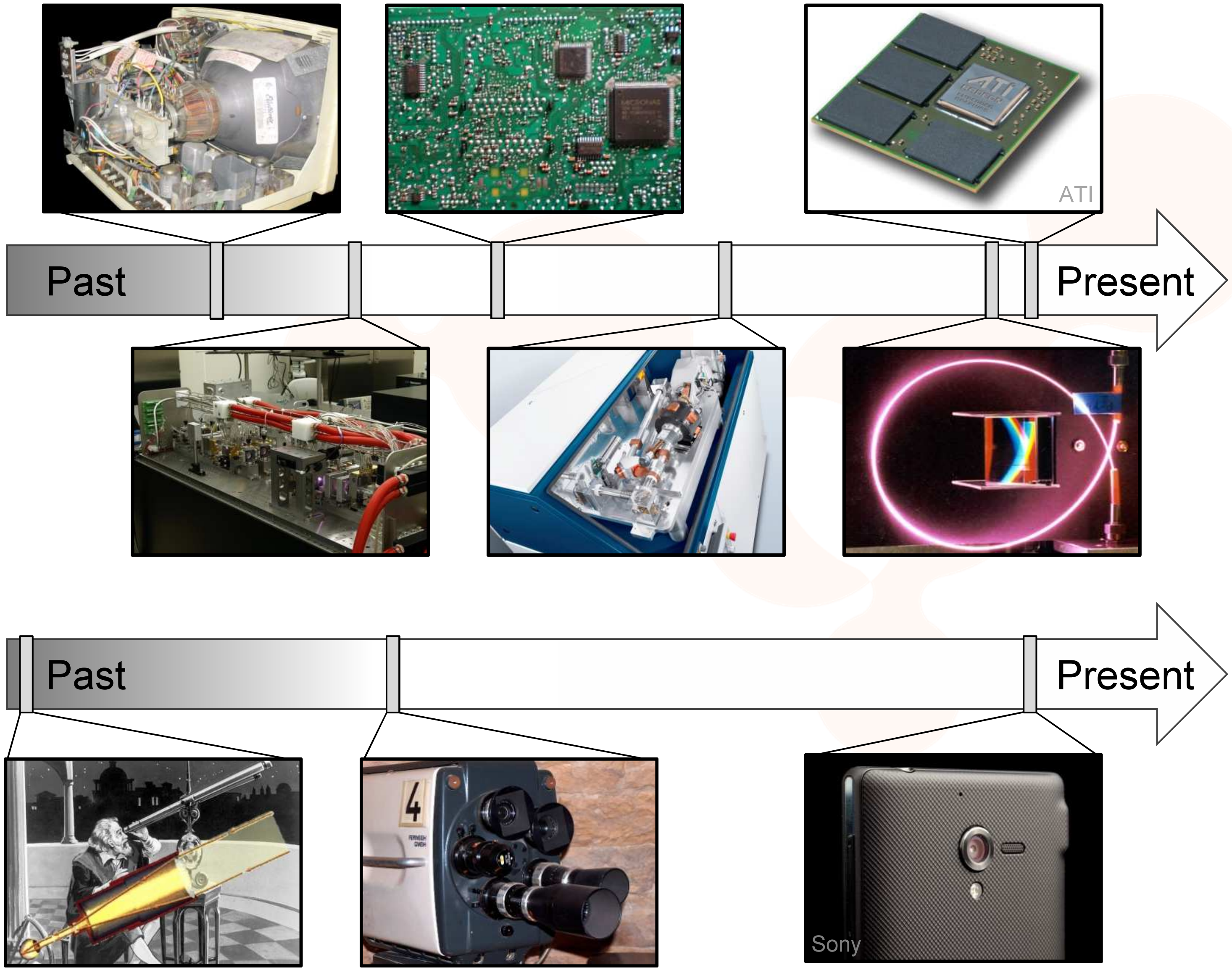

Planar integration of optics

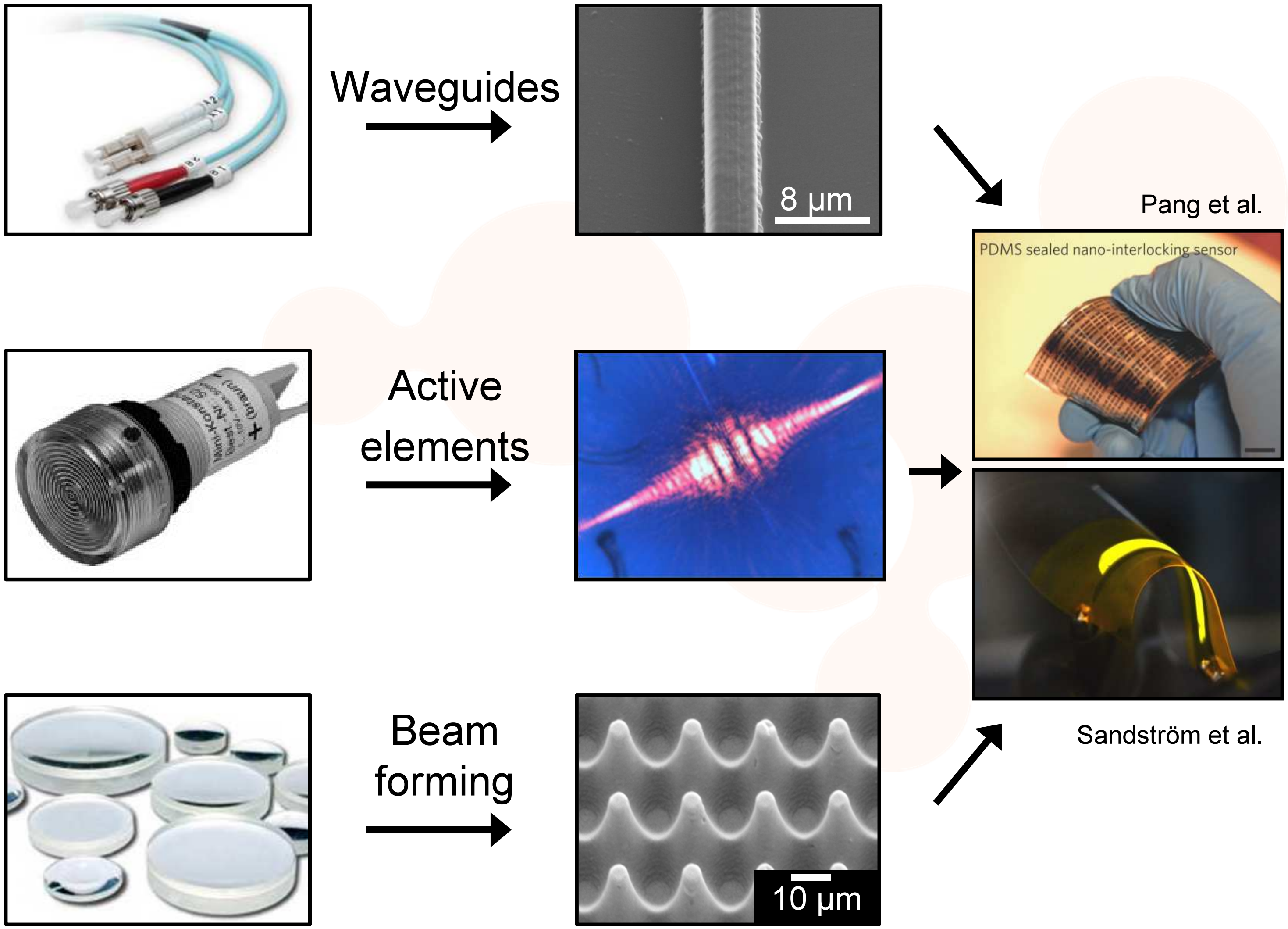

Outline

- Introduction
- **Vision of sensor concepts**
- Materials
- Production methods
- Characterization
- Summary

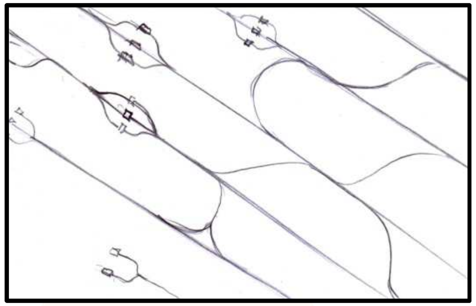

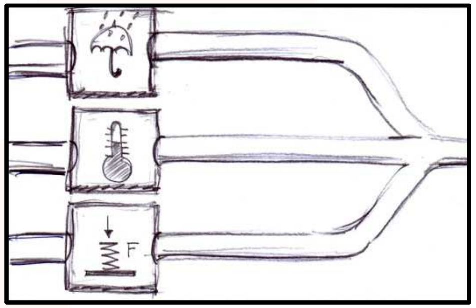

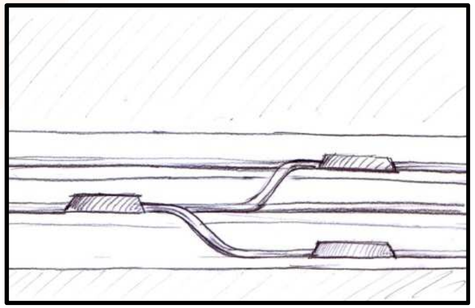

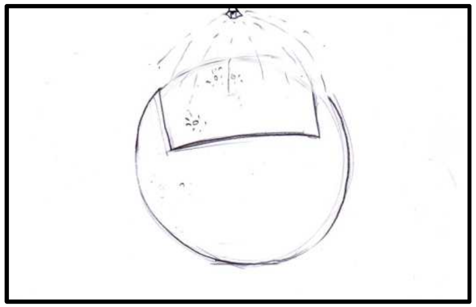

Possible and new sensor concepts

- Interferometric sensors
- Strain detection sensors
- Temperature detection sensors
- Whispering gallery mode sensors
- Planar optical polymer foil spectrometer

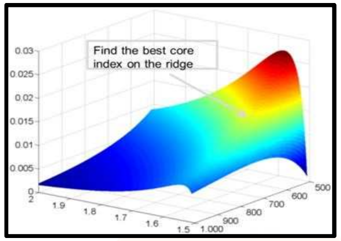

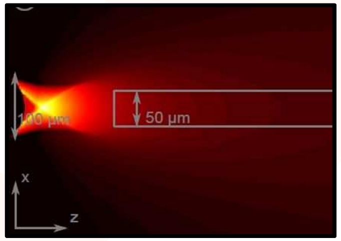

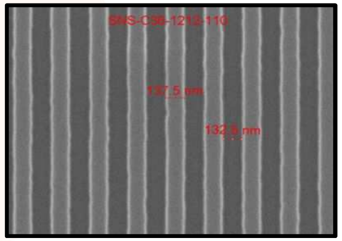

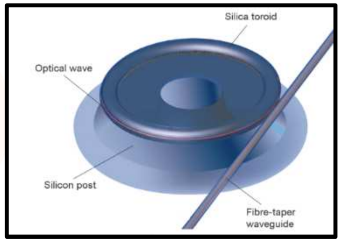

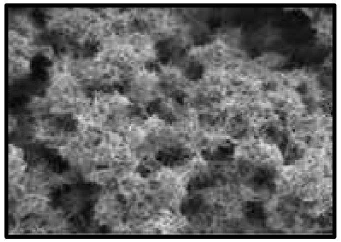

Mach-Zehnder interferometric sensor

- Simulation for two bending paths
  - ✓ Cosine function $$x(z) = h \cdot \left(\frac{z}{l} - \frac{\sin(\frac{2\pi \cdot z}{l})}{2\pi} \right)$$
  - ✓ Sine function $$x(z) = h \cdot \sin^2\left(\frac{\pi \cdot z}{2 \cdot l} \right)$$
  - ✓ $\mathrm{Loss}_{\mathrm{Cos}} < \mathrm{Loss}_{\mathrm{Sin}}$

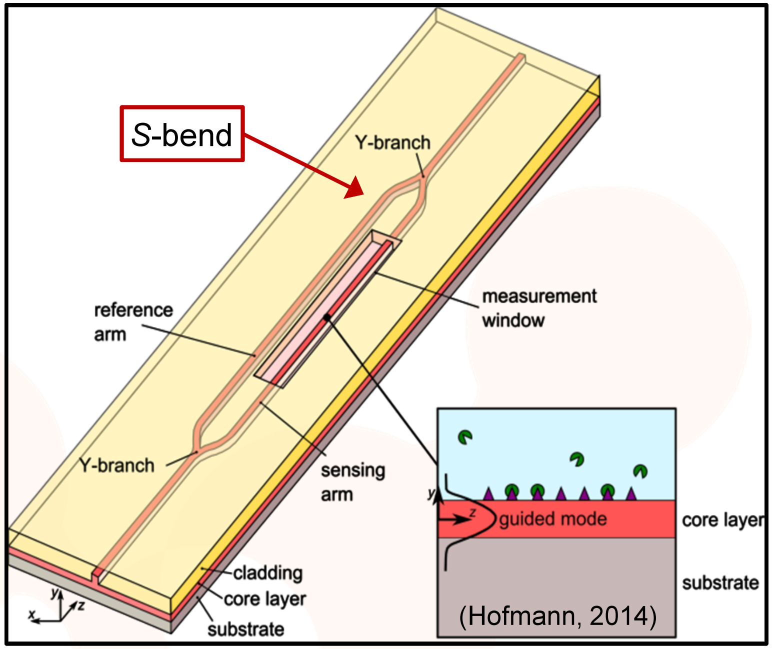

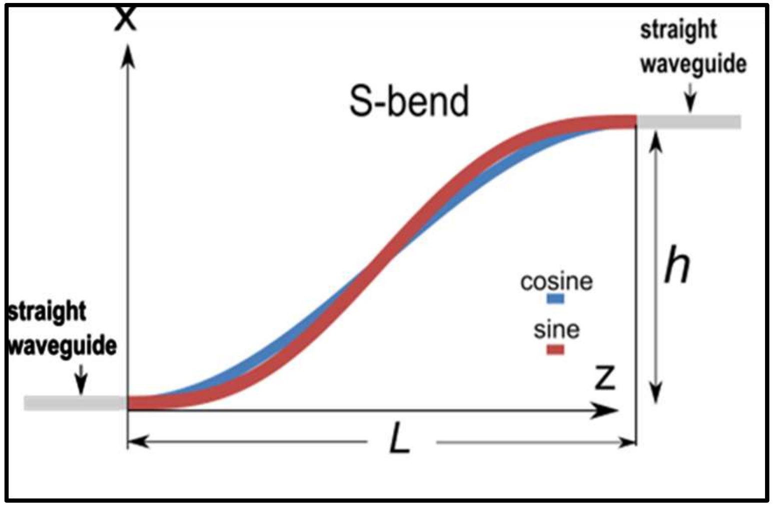

Fig. 15.1: S-bend funtions for Mach-Zehnder interferometer (Hofmann, 2014).

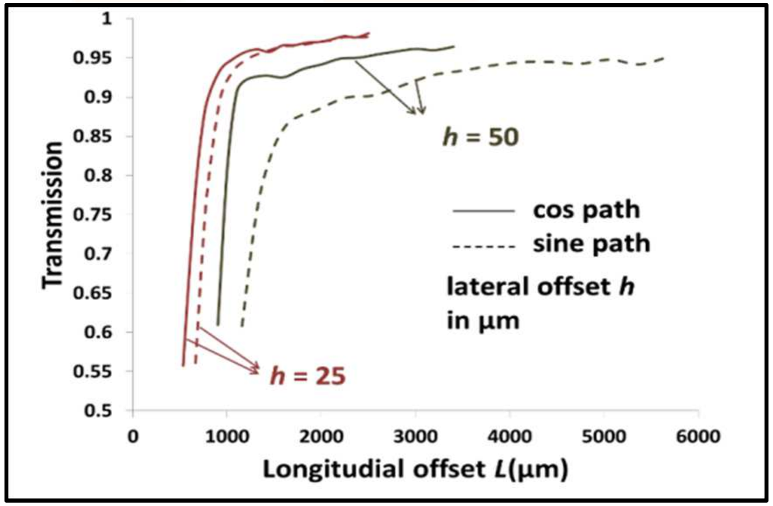

Fig. 15.2: Transmission within S-bends (Hofmann, 2014).

Planar integrated strain detection sensors

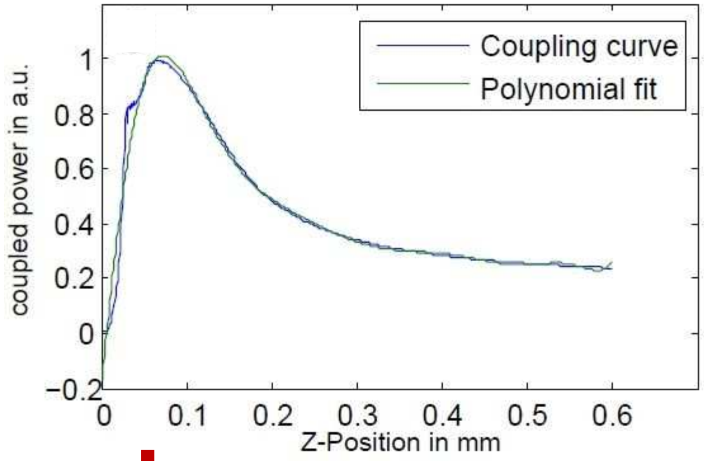

- Conversion of geometric strain into intensity modulation
- Micro-lenses focus beam
- Intensity dependent on elongation, i.e. distance to focus of beam

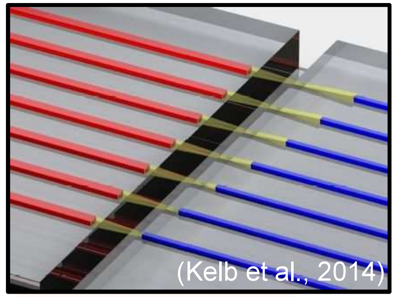

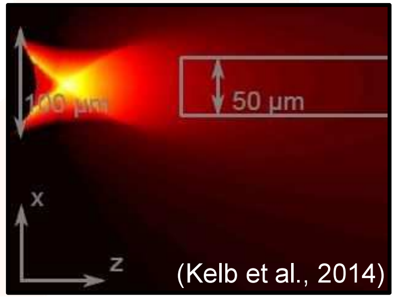

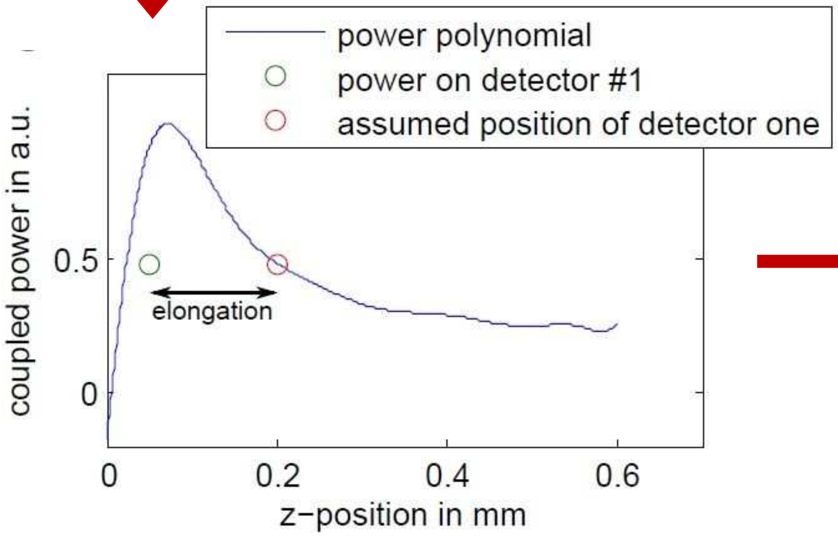

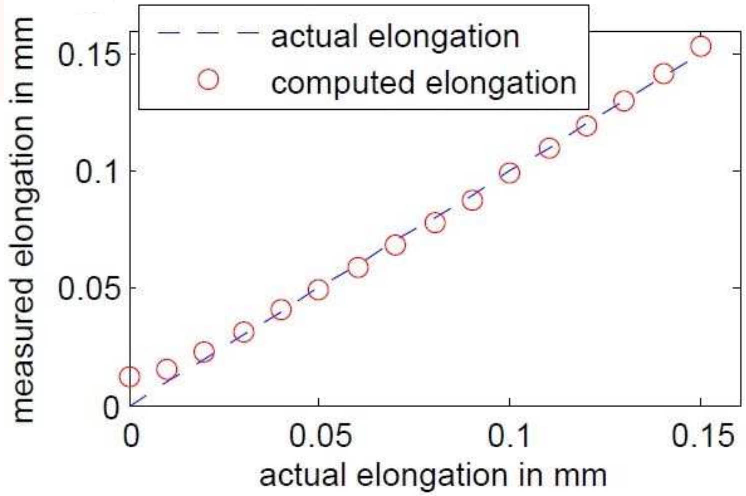

Fig. 17.1 (top, bottom left and right): Readout strategy of the strain sensor, shown for one detection waveguide (Kelb et al., 2014).

Kelb C, Reithmeier E, Roth B. Planar integrated polymer-based optical strain sensor. Proceedings of SPIE Photonics West 8977, 2014 MOEMS and Miniaturized Systems XIII, 89770Y (March 7, 2014)

Planar integrated temperature detection sensors

- Negative thermo-optic coefficient
- Positive thermal expansion

} Same order of magnitude

- Material characterization extremely important
- Small spectral shift (-7×10^{-3} nm K^{-1}) → Detection?

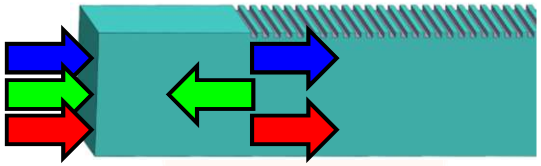

Fig. 19.1: Concept for temperature sensor based on fiber-Bragg grating (IMTEK, Freiburg).

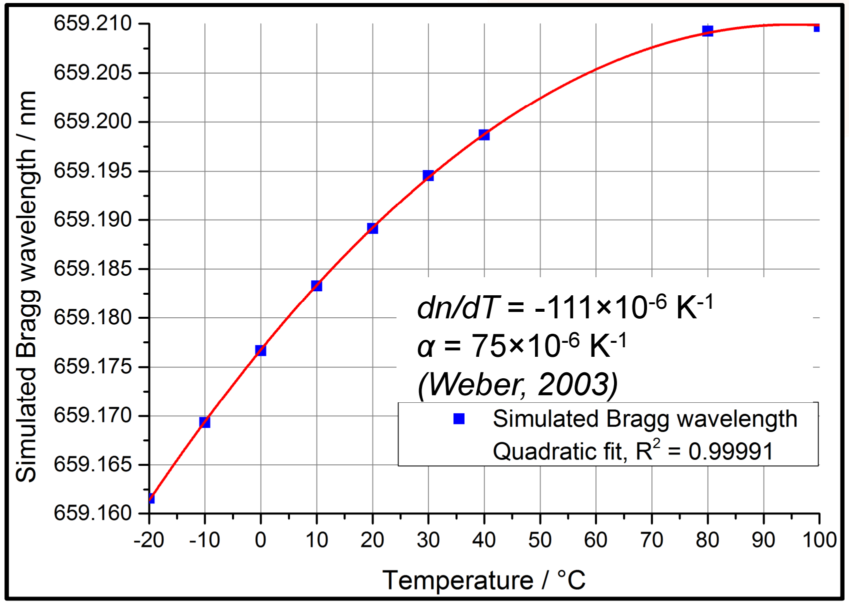

Fig. 19.2: Simulation results in PMME according to Weber (Sherman, 2014).

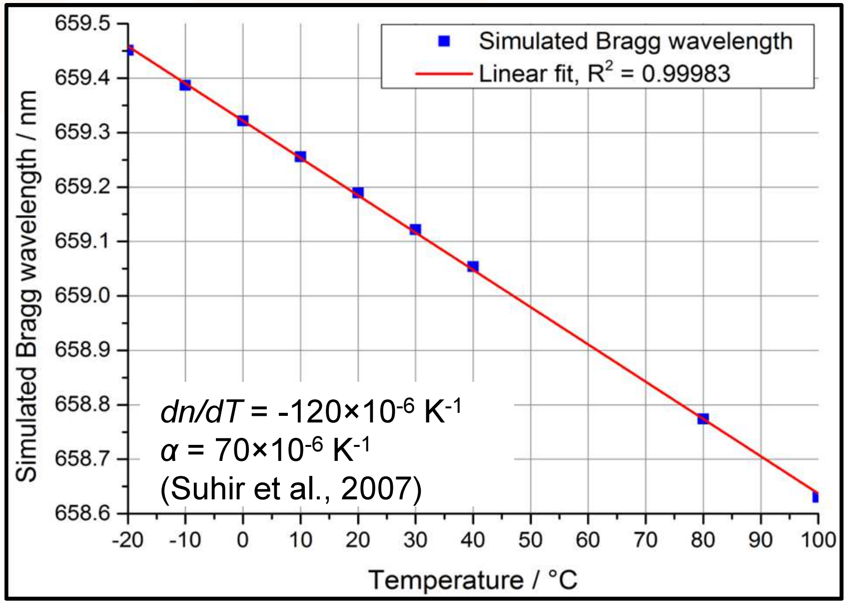

Fig. 19.3: Simulation results in PMME according to Suhir et al. (Sherman, 2014).

Suhir E., Lee Y. C., Wong C. P., Micro- and Opto-Electronic Materials and Structures: Physics, Mechanics, Design, Reliability, Packaging: Volume I, Springer, 2007.
Weber M. J. Handbook of Optical Materials, CRC Press, 2003.

Whispering gallery mode resonators

- Foil integrated Whispering-gallery mode sensors
- Resonant frequencies very sensitive to changes on surrounding refractive index
- Ultimate target sensitivity: single-molecule detection in liquid phase

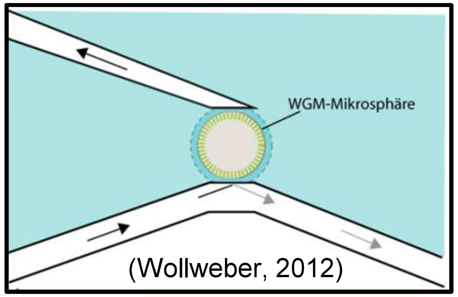

Figure 20.1: The microsphere is attached to one waveguide, another waveguide detects the transmitted signal.

- Simulation with RSoft
  - ✓ Ring-resonator: inner diameter 4.5 µm, thickness 1 µm, n=1.59
  - ✓ The left waveguide is used as an excitation source: thickness 1 µm, n=1.46
  - ✓ In case of resonance: light is coupled into the ring-resonator, dip in the transmission signal

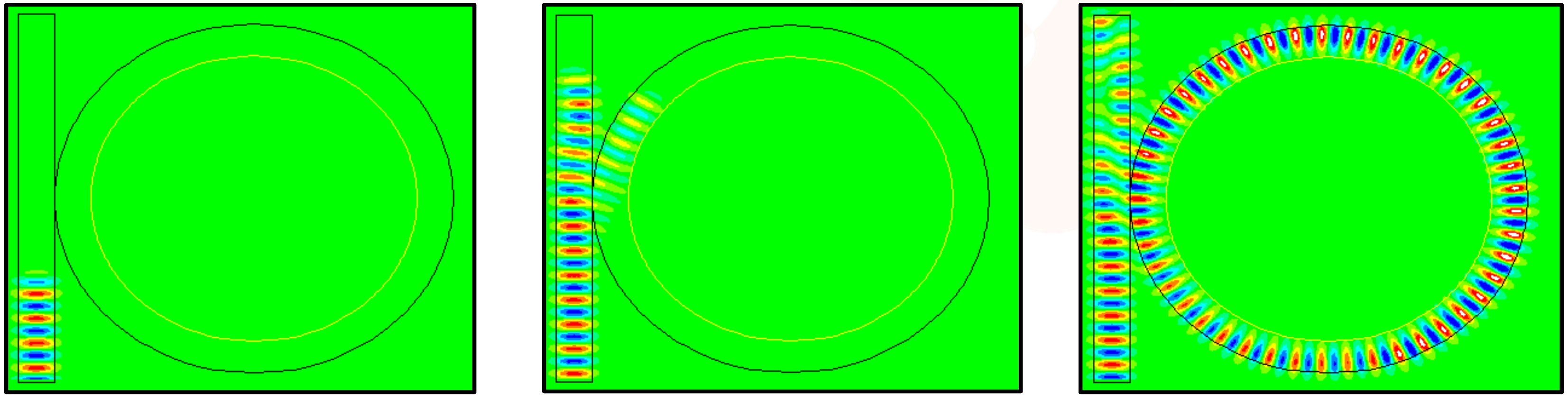

Figure 20.2: Build-up of the electromagnetic field in the WGM of a 1 µm thick ring resonator, λ = 1089 nm (Petermann, 2014).

Planar optical polymer foil spectrometer - PolyAWG

- Simulations for singlemode waveguides
- Singlemode waveguide cores with either high aspect ratio or small dimensions (< 700 nm)
- ZnO nanowires in substrate against mechanical strain

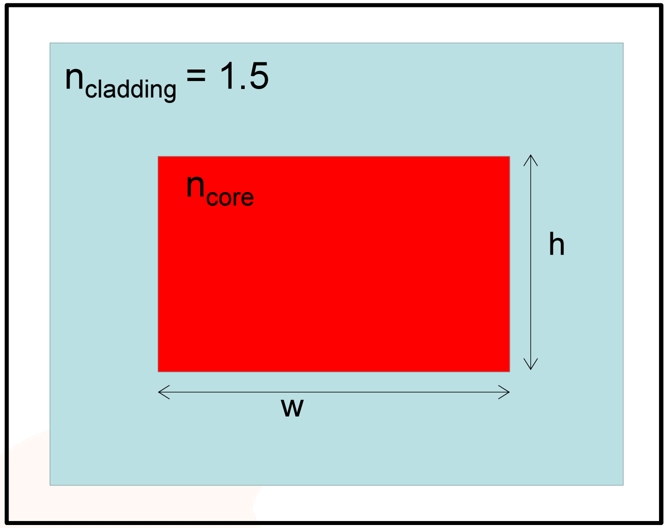

Fig. 21.2: Geometry (height x width) of the simulated waveguides (TU Clausthal).

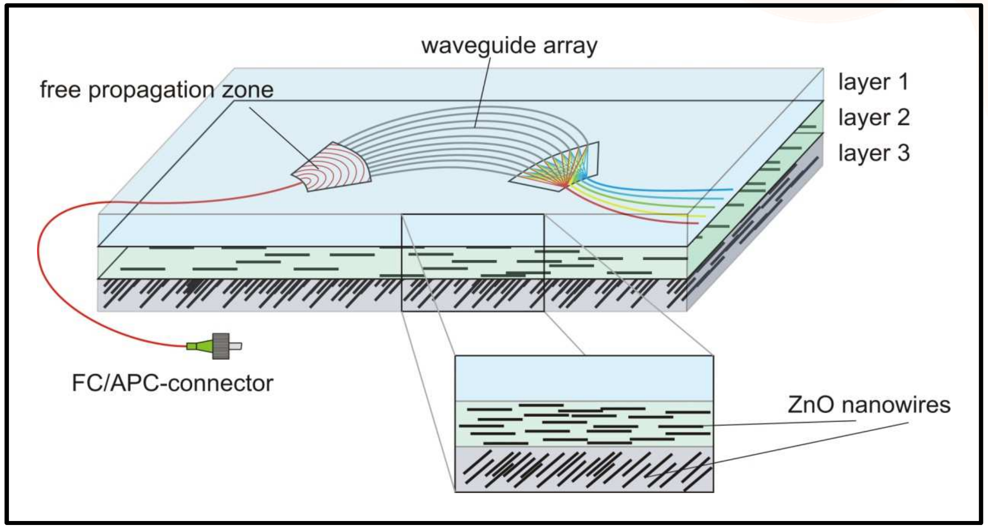

Fig. 21.1: Sketch of an AWG (TU Clausthal).

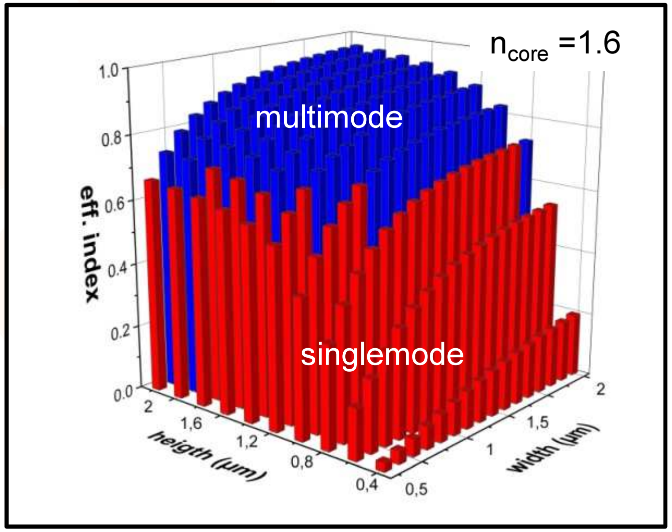

Fig. 21.3: Simulations performed with PhotonDesing® FIMMWAVE, red bars represent the single-mode region (TU Clausthal).

Koch J., Angelmar M., Schade W.: Arrayed waveguide grating interrogator for fiber Bragg grating sensors: measurement and simulation AO, Vol 51, 7718-7723 (2012).

Outline

- Introduction
- Vision of sensor concepts
- **Materials**
- Production methods
- Characterization
- Summary

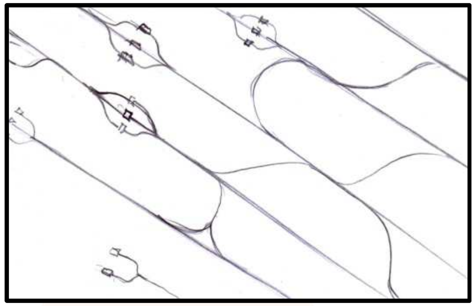
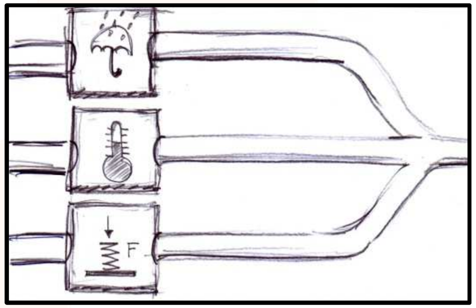
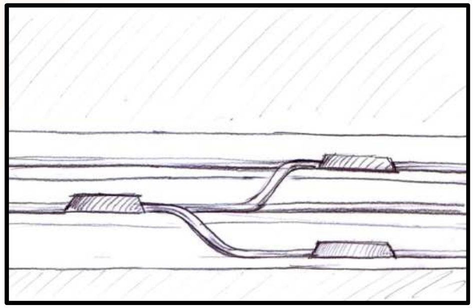
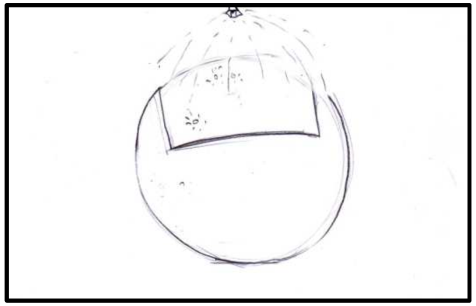

We need tailored polymers!

- **Target**
  - ✓ Development of polymers with tailored optical & thermo-mechanical properties for polymer waveguides

- **Concept**
  - ✓ Prepolymer synthesis with respect to
  - ✓ adjustable physical properties
  - ✓ use in a variety of shaping/molding techniques

- **Prepolymer**
  - ✓ adjustable viscosity (10^{-3} – 10^{2} Pa•s)
  - ✓ UV/Vis curing favorable

- **Polymer**
  - ✓ adjustable refractive index (1.39 < n < 1.65 @ 589 nm)
  - ✓ optical damping less than 1 dB/m
  - ✓ continuous operation temperature > 100°C

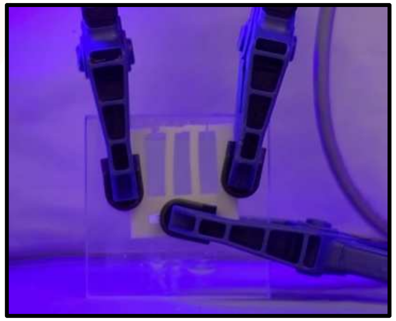

Refractive index tailored hybrid polymers

- Prepolymer → MMA/PMMA/1,3-Butandioldimethacrylate (BDMA)
- Polymer → Poly(methylmethacrylate-co-1,3-butandioldimethacrylate)
- Dopant → Phenanthrene

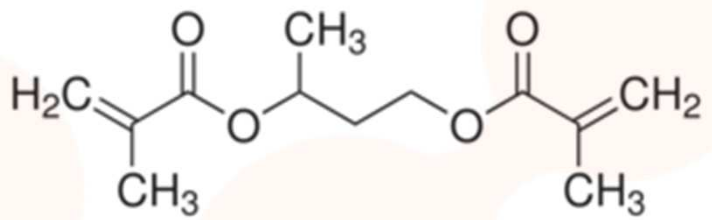

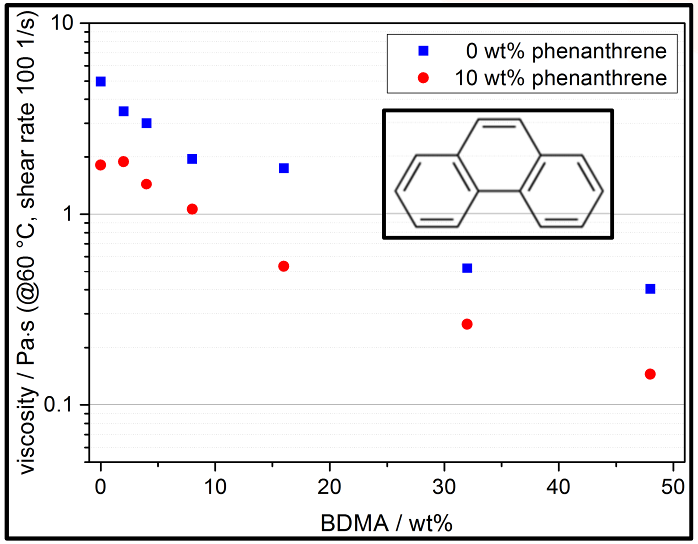

Fig. 25.1: Viscosity adjustment with prepolymer concentration, 5 Pa·s > η > 0.15 Pa·s, @100 1/s, 60°C (IMTEK, Freiburg).

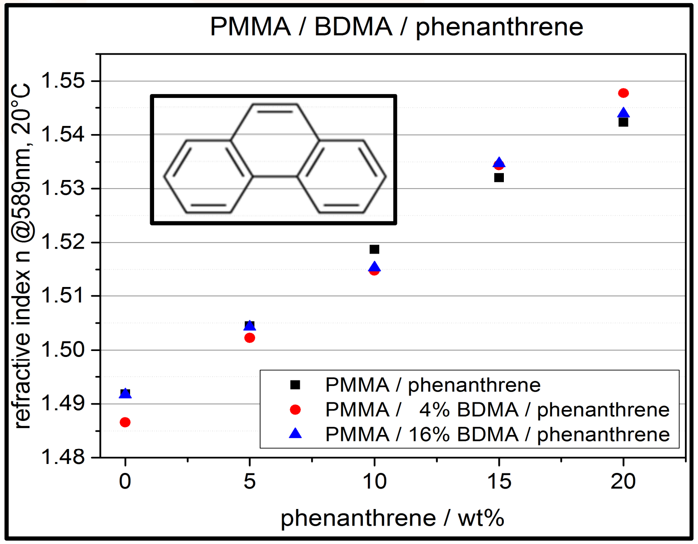

Fig. 25.2: Refractive index change with dopant concentration, 1.49 < n < 1.55, @589 nm, 20 °C (IMTEK, Freiburg).

Outline

- Introduction
- Vision of sensor concepts
- Materials
- **Production methods**
- Characterization
- Summary

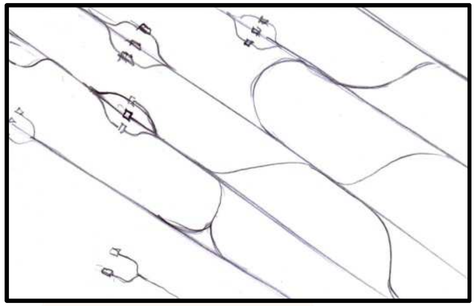

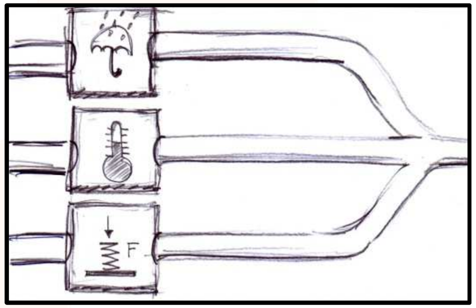

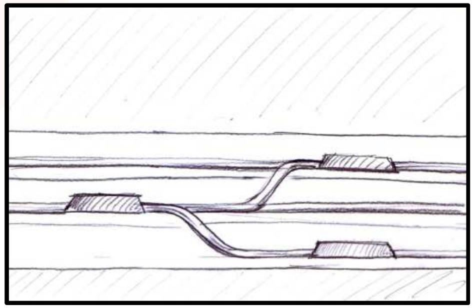

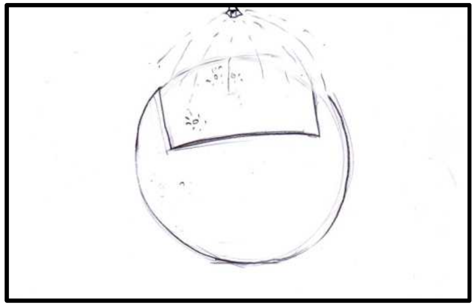

A view on a starting setup

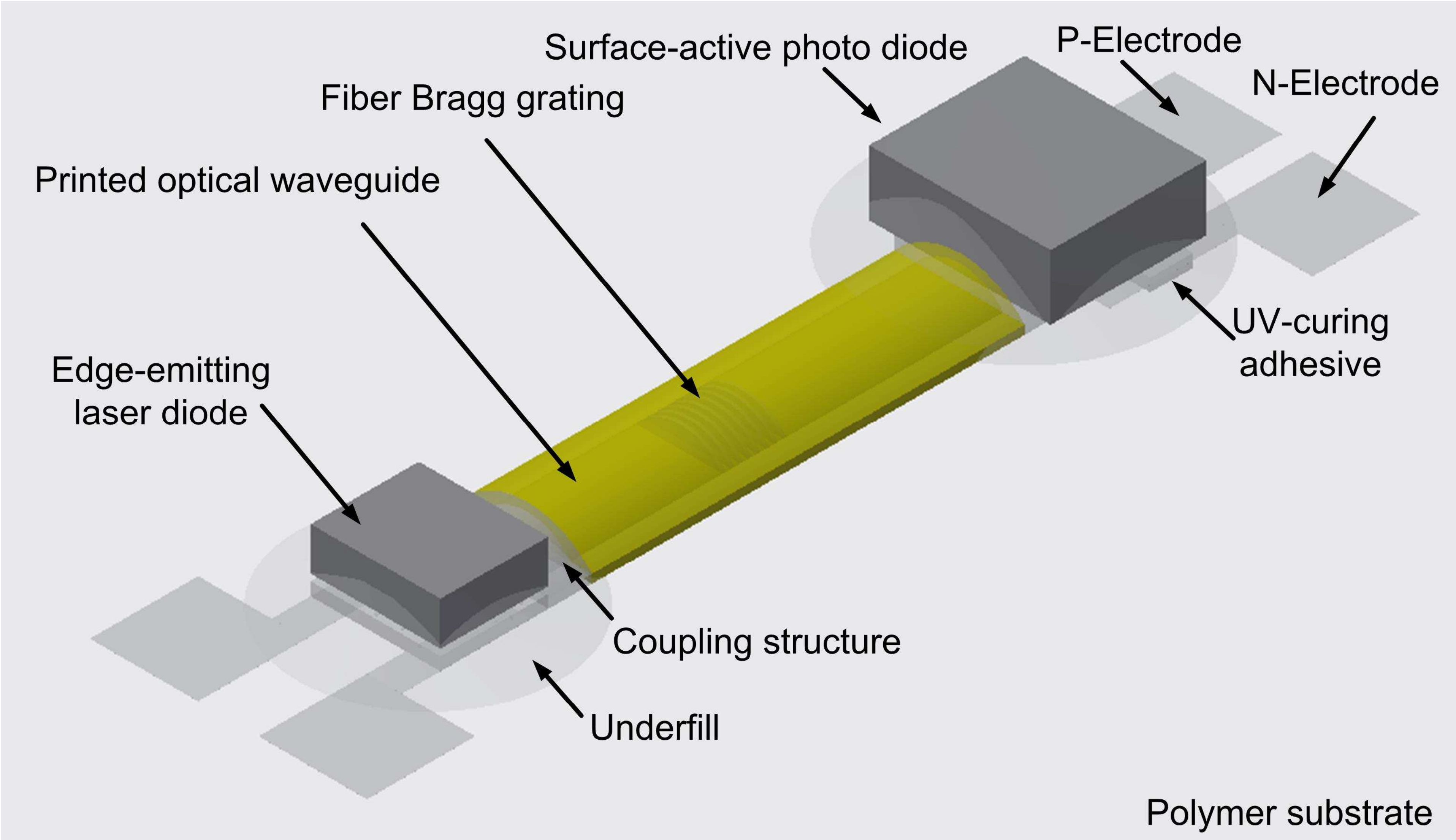

Fig. 29.1: Planar optronic sensor system; highlighted waveguide (Wang, 2014).

* Wang, Y., L. Overmeyer, „Low temperature Optodic Bonding for Integration of Micro Optoelectronic Components in Polymer Optronic Systems", Procedia Technology, Elsevier, (accepted).

Production concepts for integrated waveguides

- Laser processes
  - ✓ fs- laser processing
  - ✓ UV-photolithograghy

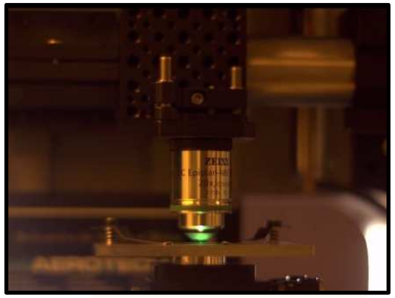

- Hot embossing and nano imprint

- Printing
  - ✓ Offset
  - ✓ Flexographic
  - ✓ Inkjet

- Lamination and surface coating

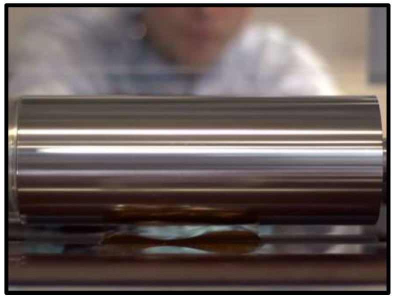

Polymer processing with fs-laser and UV-lithography

Two-Photon-Polymerization (2PP)

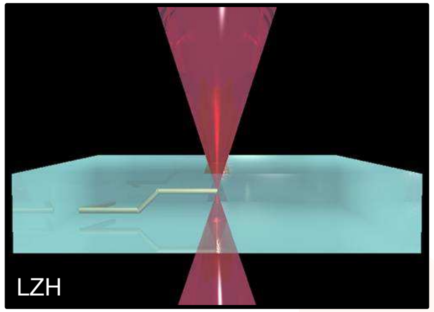

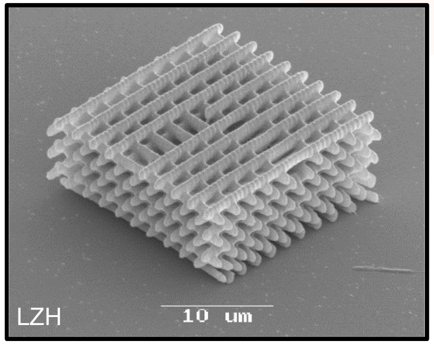

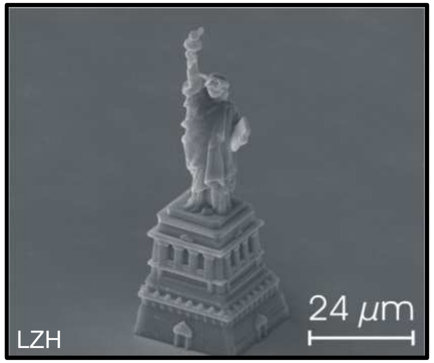

Microscope Projection Photolithography (MPP)

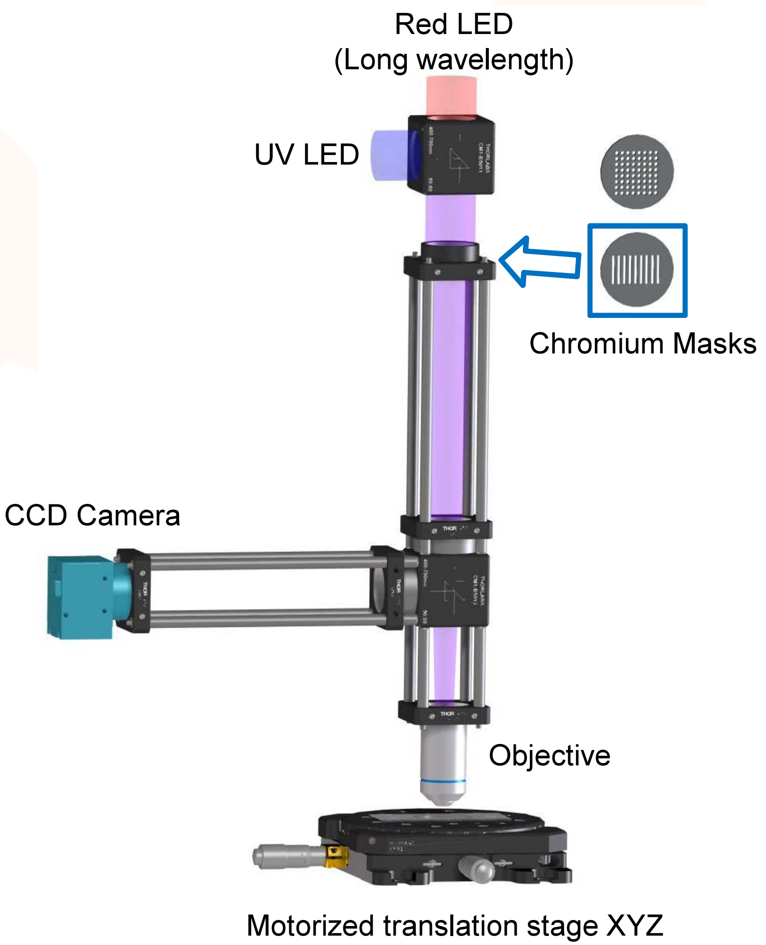

2PP vs. MPP

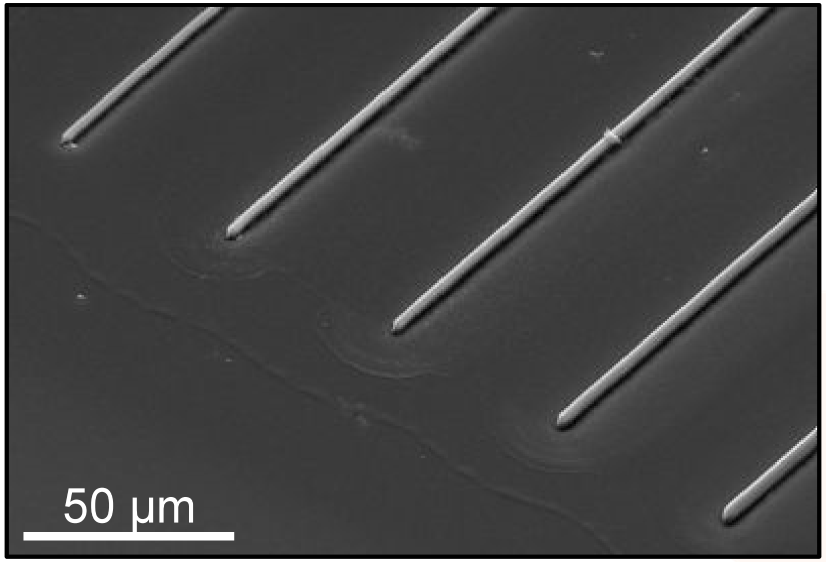

Fig. 33.1: Polymer waveguides on a glass substrate (Zywietz, 2014).

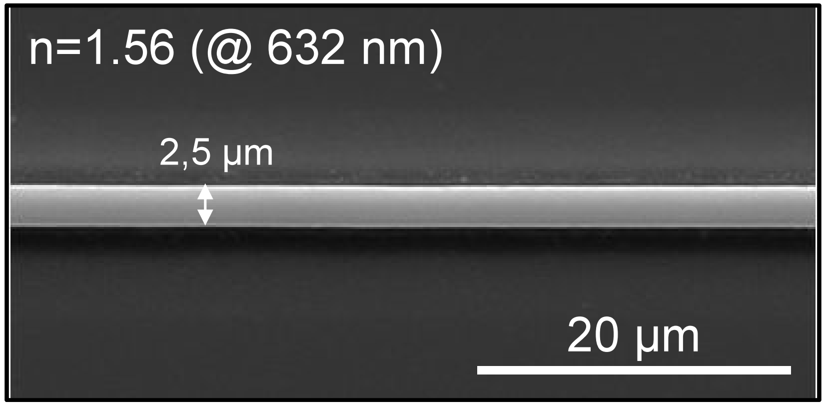

Fig. 33.2: Single polymer waveguide fabricated by 2PP (Zywietz, 2014).

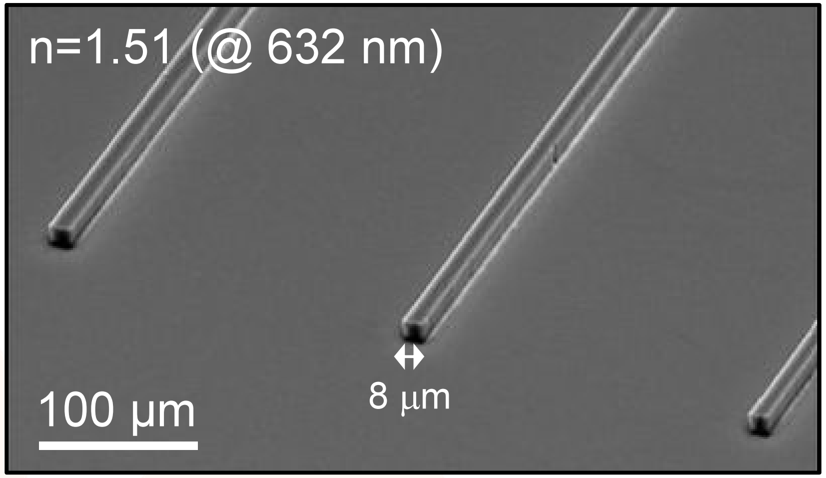

Fig. 33.3: SEM-image of MPP generated polymer waveguides (Zywietz, 2014).

Fig. 33.4: Polymer waveguides on a highly flexible PMMA substrate (Zywietz, 2014).

*Zywietz, U., C. Reinhardt, A.B. Evlyukhin, B.N. Chichkov, „Laser printing of silicon nanoparticles with resonant optical electric and magnetic responses“, Nature Communications, 5, No. 3402, (2014).

Hot embossing of micro-optical components

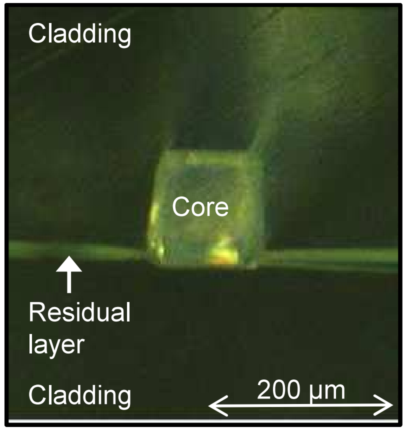

Fig. 34.1: Fabricated optical waveguides through hot embossing (Rezem, 2014).

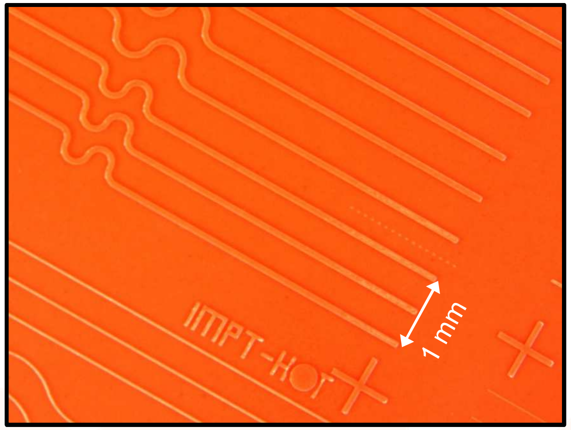

Fig. 34.2: Waveguide structures on a silicone embossing stamp (Rezem, Akin, 2014)

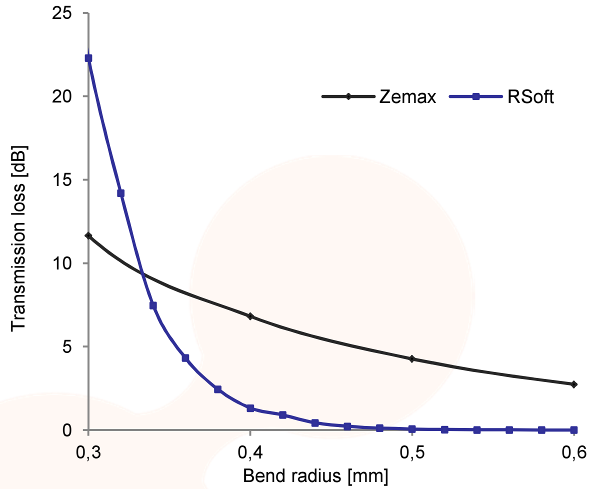

Fig. 34.3: Waveguide transmission losses as a function of the bend radius simulated in Zemax and RSoft (Rezem, 2014).

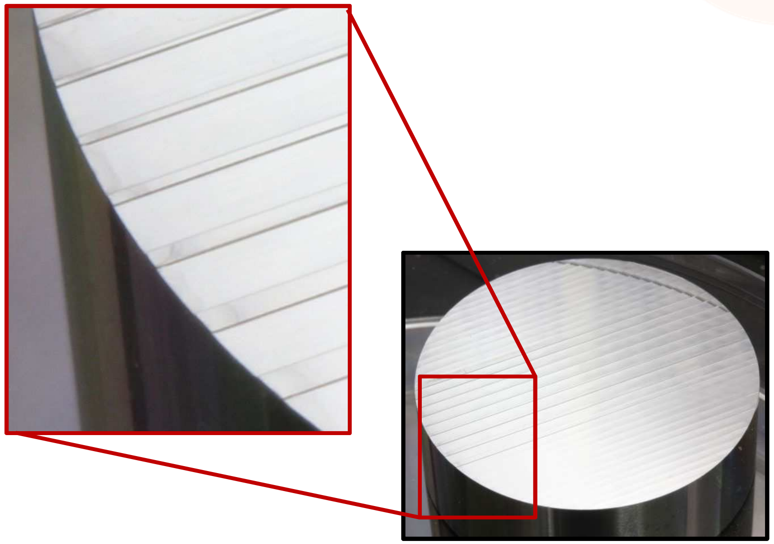

Fig. 34.4: Hot-embossing tool currently under development (Kelb, 2014).

- Manufacturing of coupling structures and waveguides in 350 µm-thin polymer foils
- Different coupling structures have been tested

Rezem, M., A. Günther, M. Rahlves, B. Roth, and E. Reithmeier, „Hot embossing of polymer optical waveguides for sensing applications“, Procedia Technology, Elsevier, (accepted).

High throughput production of optical waveguides

- Demand: Manufacture of planar waveguide network on polymer foil

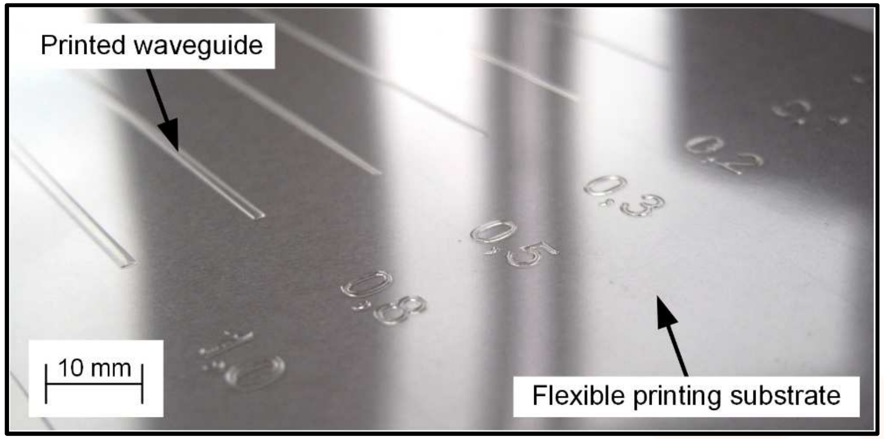

Fig. 35.1: Flexographic printed waveguides; acrylate on PVC substrate (Wolfer, 2013).

- Process requirements for large scale production:
  - ✓ high throughput
  - ✓ high resolution

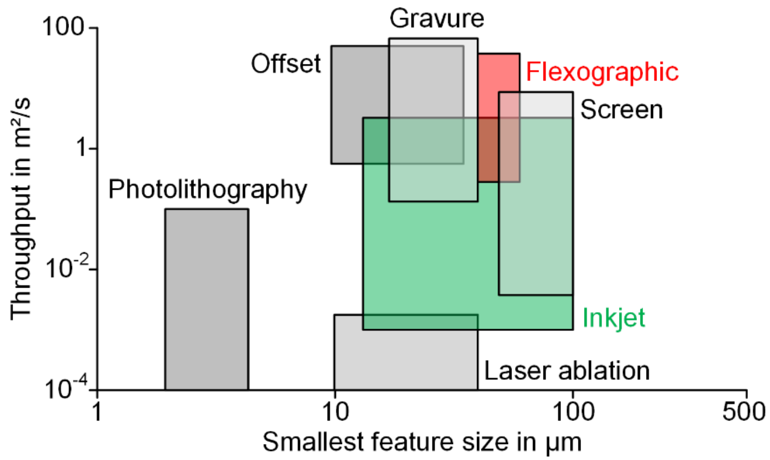

Fig. 35.2: Process limits of printing methods (OE-A Roadmap).

- Approach:
  Combination of two printing processes
  - ✓ Flexographic printing for prestructuring of films with high throughput
  - ✓ Inkjet printing for individual complement with high resolution

Wolfer, Bollgruen, Mager, Overmeyer, Korvink (2014). Flexographic and inkjet printing of polymer optical waveguides for fully integrated sensor systems. Technology Procedia, Elsevier.

OE-A Roadmap for Organic and Printed Electronics, 5th ed., VDMA Verlag, 2013

High throughput production of optical waveguides

- Flexographic printing machines
  - ✓ Process development in laboratory scale
  - ✓ Verification on modified industrial scale printing machine

Fig. 36.1: Flexographic printing machine in laboratory scale, IGT F1 UV

Fig. 36.2: Printing machine Speedmaster SM52 (Source: Heidelberger Druckmaschinen AG).

- Inkjet printing machines

Fig. 36.3: Pixdro LP 50 (Source: Meyer Burger)

Fig. 36.4: Dimatix DMP 2831 (Source: Dimatix)

OE-A Roadmap for Organic and Printed Electronics, 5th ed., VDMA Verlag, 2013

High throughput production of optical waveguides

- Typical properties of printed multimode optical waveguides

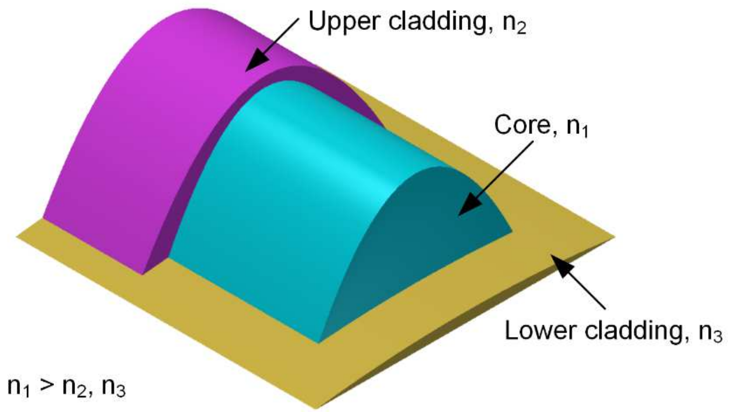

Fig. 38.1: Computed 3D model of printed waveguide (Wolfer, 2013).

Table 2: Typically achieved process properties (Wolfer, 2014).

Property	Value
Width	20-1,000 µm
Height	4-110 µm
Max. aspect ratio	0.5
Speed of operation	50-260 m²/h
Surface roughness	12.5 nm

- Waveguide setup in layers with parabolic shape

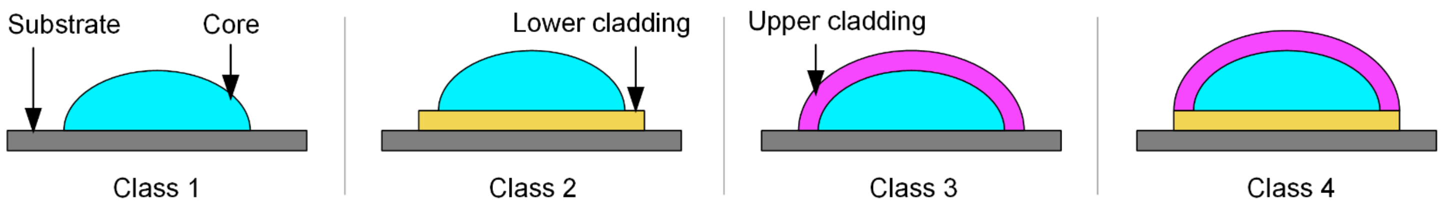

Fig. 38.2: Possible waveguide concepts by combining the core and cladding layers (Wolfer, 2014).

Wolfer, Bollgruen, Mager, Overmeyer, Korvink (2014). Flexographic and inkjet printing of polymer optical waveguides for fully integrated sensor systems. Technology Procedia, Elsevier.

What about active optical systems?

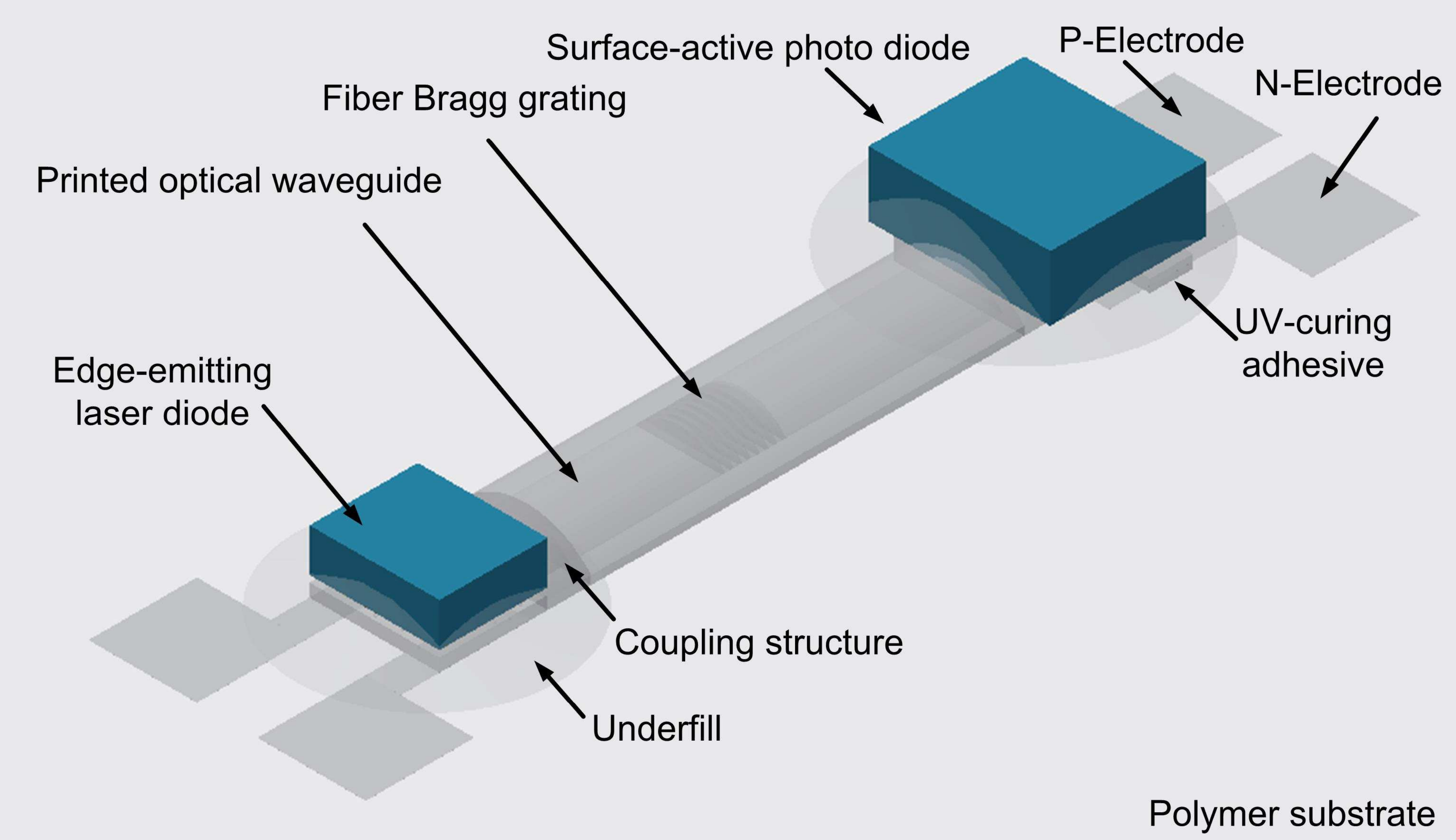

Fig. 43.1: Planar optronic sensor system; highlighted diodes (Wang, 2014).

Optodic bonding as bridging technology

- High success rate
  → 95 %
- Short process time
  → app. 10 s
- Mechanical strength
  → 23 N/mm²

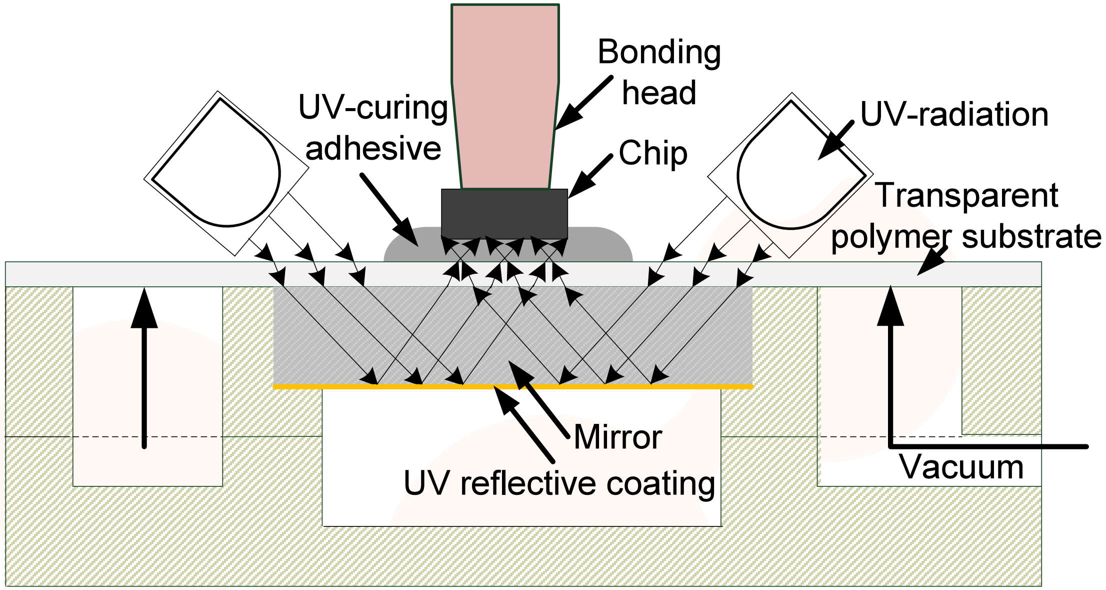

Fig. 44.1 (right)**:** Schematic illustration of optode for sideway irradiation (Wang, 2014)

- Electrical conductivity

✓ panacol 4732:	0.292 Ω
✓ Dymax OP-29:	0.169 Ω
✓ Dymax OP-29-Gel:	0.112 Ω
✓ Dymax OP-24-Rev-B:	0.110 Ω
✓ Delo GB368:	0.286 Ω

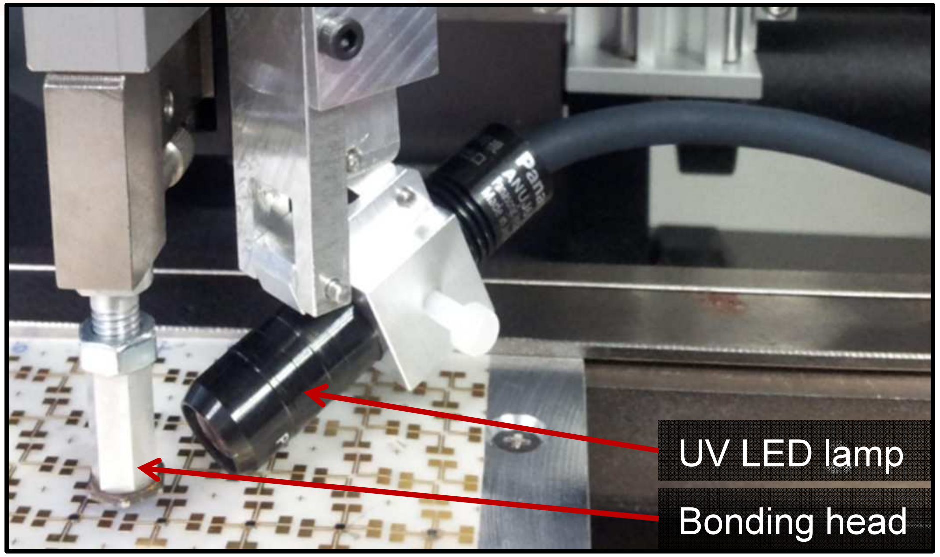

Fig. 44.2: Photo of realized optode, (Low Temperature Optodic Bonding for Integration of Micro Optoelectronic Components in Polymer Optronic Systems, Wang et al., SysInt 2014, accepted).

Integration of OLEDs and OPDs into waveguide systems

- Waveguide integrated device for detection at 634 nm
  - ✓ ITO on polymer waveguide
  - ✓ Structure optimization for high responsivity

- Optical simulations of OPD/waveguide structures
  - ✓ Mode distribution
  - ✓ Waveguide losses (loss channels)

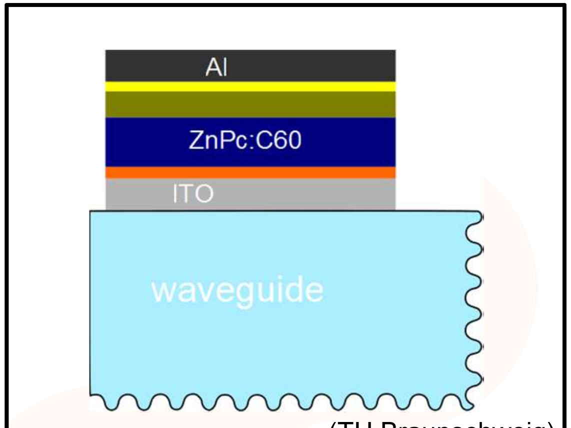

(TU Braunschweig)

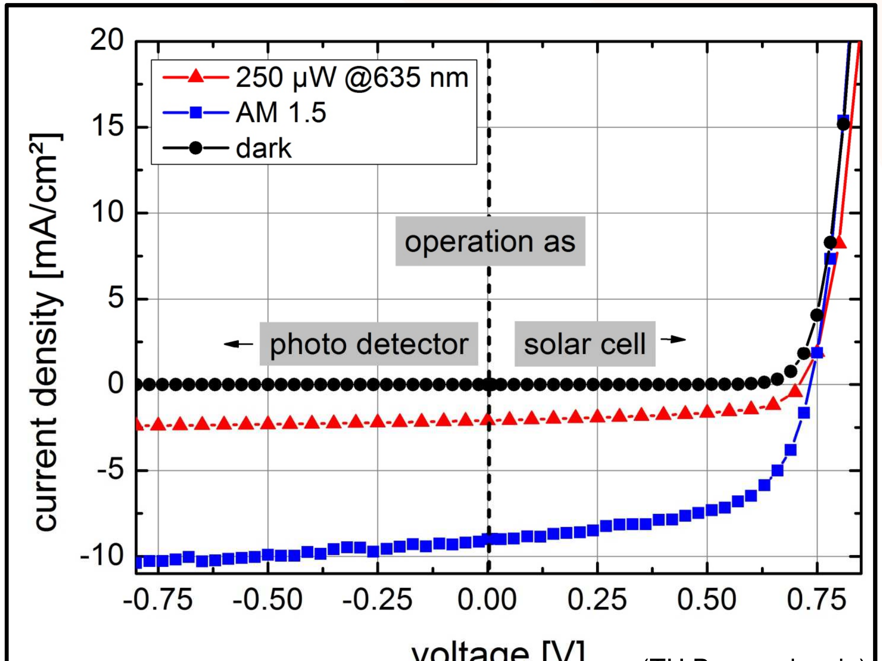

(TU Braunschweig)

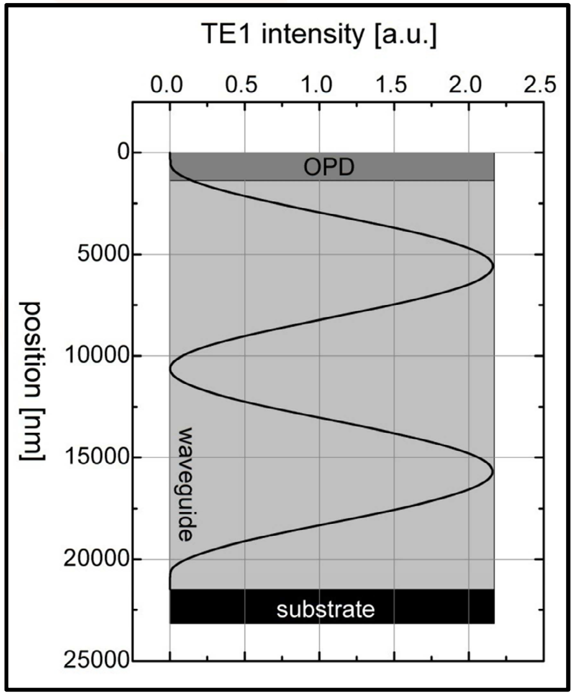

(TU Braunschweig)

Photodetector operation parameters

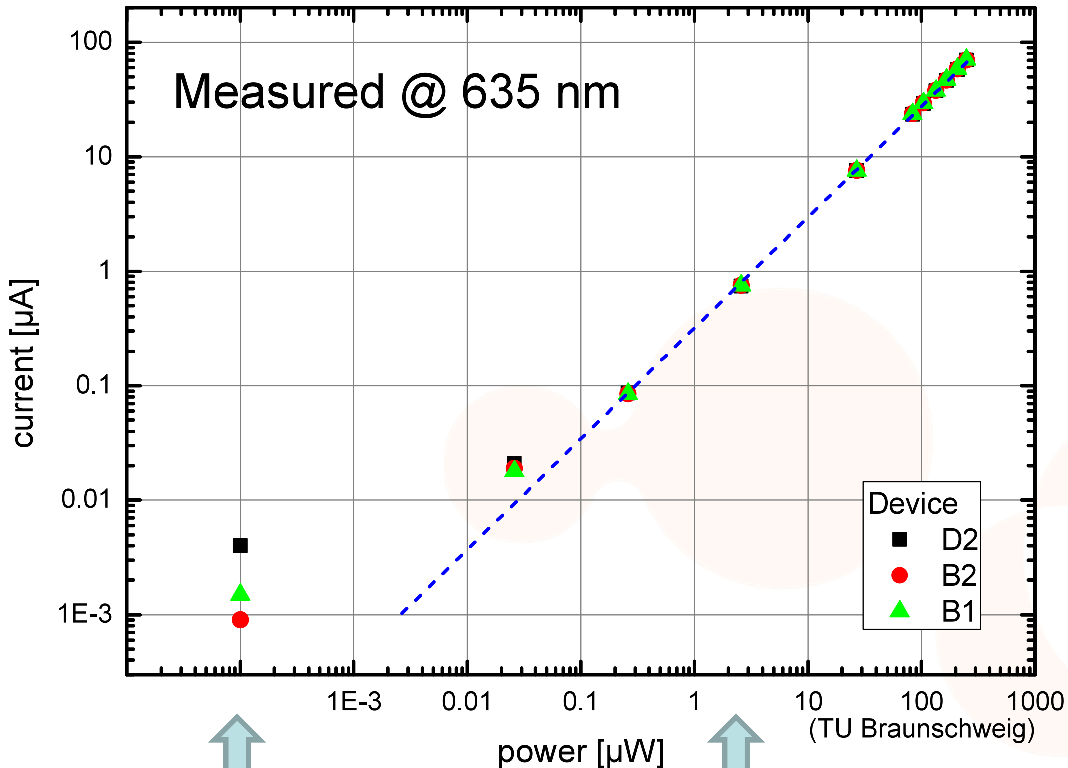

(TU Braunschweig)

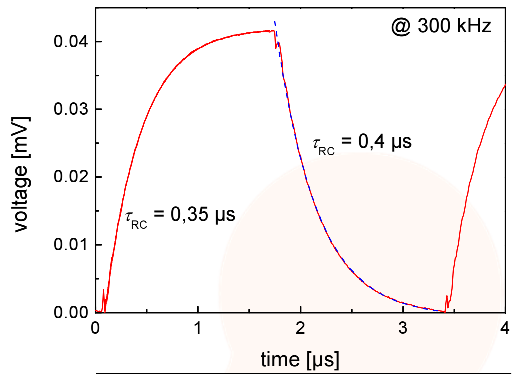

(TU Braunschweig)

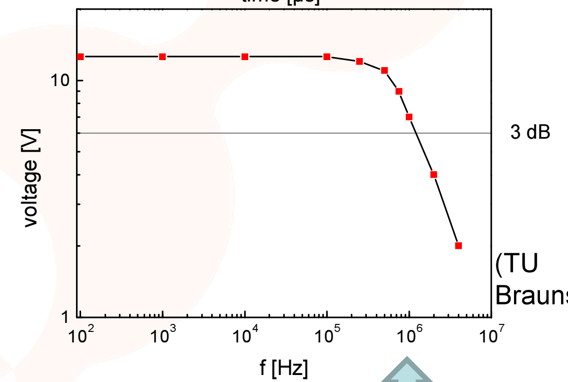

(TU Braunschweig)

Dark current:
1 nA (best)
= 33 nA/cm²

Responsivity:
320 mA/W @ -1V
63% EQE, commercial
Si ~ 80%

Bandwidth:
1 MHz
(limited by setup)

T. Otto, T. Rabe, S. Döring, W. Kowalsky, "Organic Solar Cells as Polymer Waveguide integrated Photodetectors", Procedia Technology, 2014, (accepted)

Laser-active waveguides

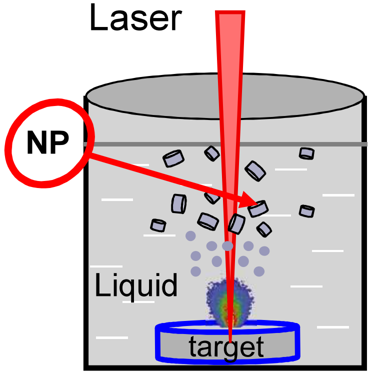

Fig. 48.1: Laser-active nanoparticle generation (Sajti, 2013).

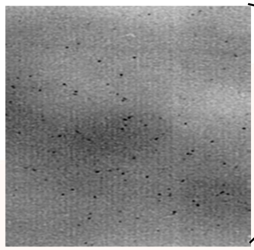

Fig. 48.2: Homogenous particle embedding (Sajti, 2013).

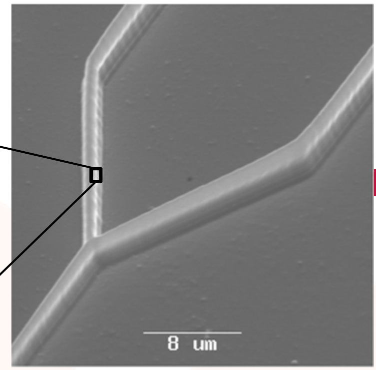

Fig. 48.3: Laser-active polymer waveguide (Sajti, 2013).

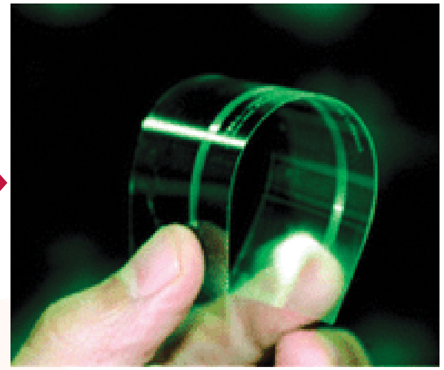

Fig. 48.4: Flexible laser module (Kwon et al., 2008).

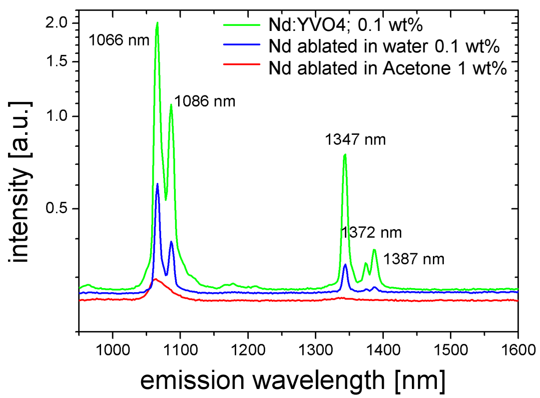

Fig. 48.5: Laser-active particles in colloidal (Sajti, 2013). form

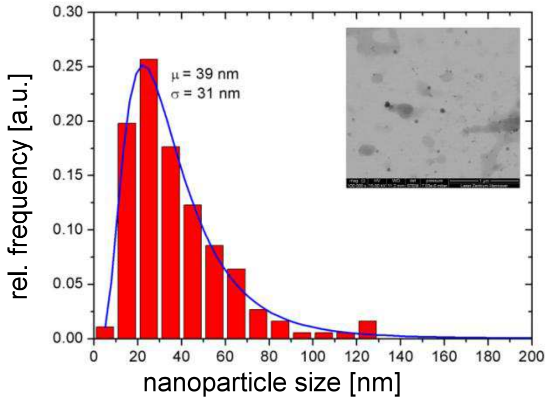

Fig. 48.6: Size distribution of laser-active particles (Sajti, 2013).

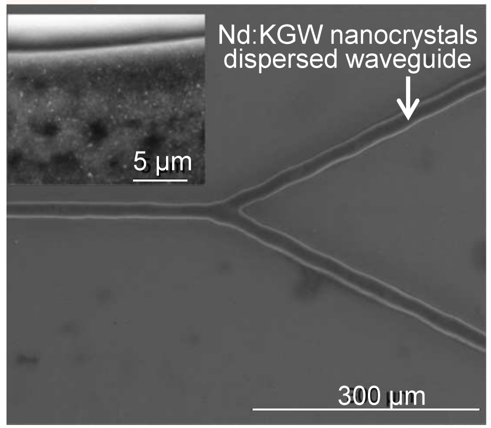

Fig. 48.7: SEM-image of Nd:KGW embedded ormosil waveguide (Sajti, 2013).

Kwon, Y.K., J.K. Han, J.M. Lee, Y.S. Koo, J.H. Oh, H.-S. Lee, E.-H. Lee, „Organic–inorganic hybrid materials for flexible optical waveguide applications", J. Mater. Chem., 18, 579-585, DOI: 10.1039/B715111J, (2008).

Outline

- Introduction
- Vision of sensor concepts
- Materials
- Production methods
- **Characterization**
- Summary

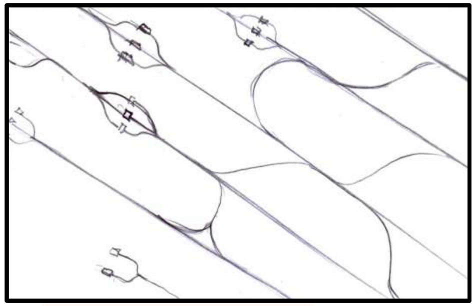

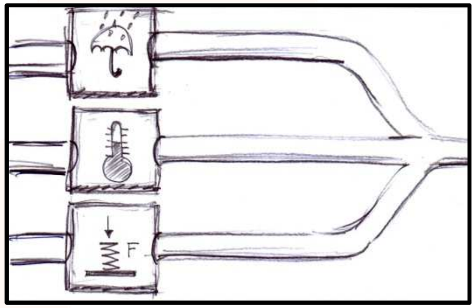

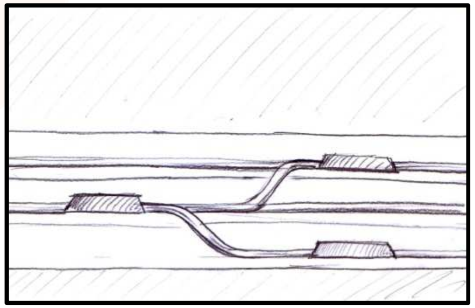

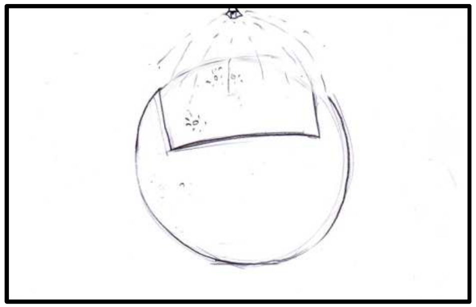

Measurement of optical transmission properties

- Attenuation of waveguides
- Refraction index distribution
- Light dispersion in waveguides
- Coupling efficiency between interfaces

⇒ Some examples of spectral measurement equipment

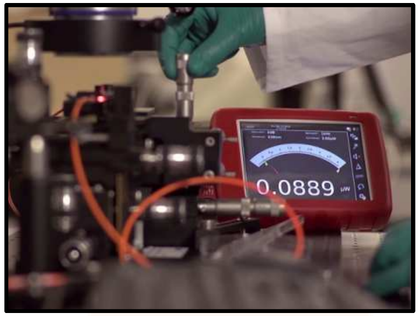

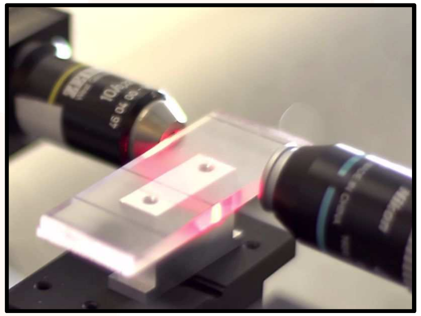
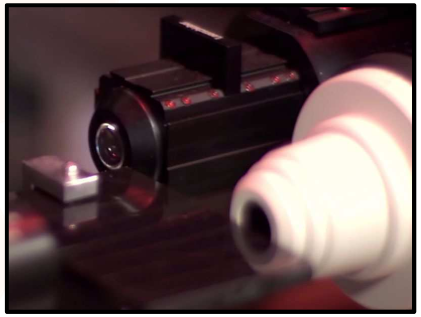
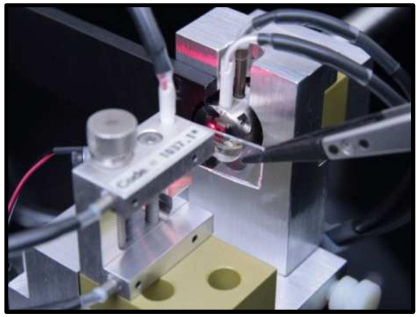

Identification of length-independent attenuation

- Light sources
  - ✓ **LED**, including confocal pattern for end face characterization
  - ✓ **Diode laser** (638 nm, 140 mW)

- Numerical aperture stapless variable within 0.1-0.5

- Aperture sizes: 1-1,000 μm

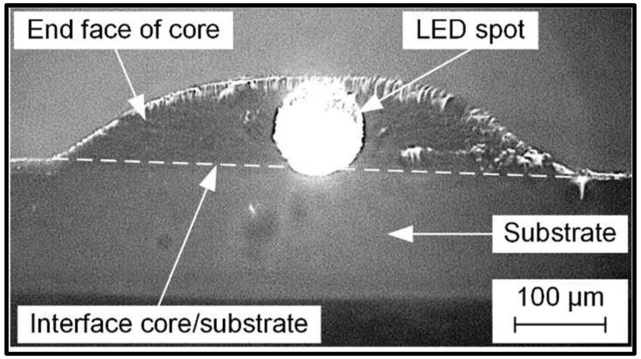

Fig. 51.1: End face of printed waveguide in optical measurement setup with focused LED spot (Wolfer, 2014).

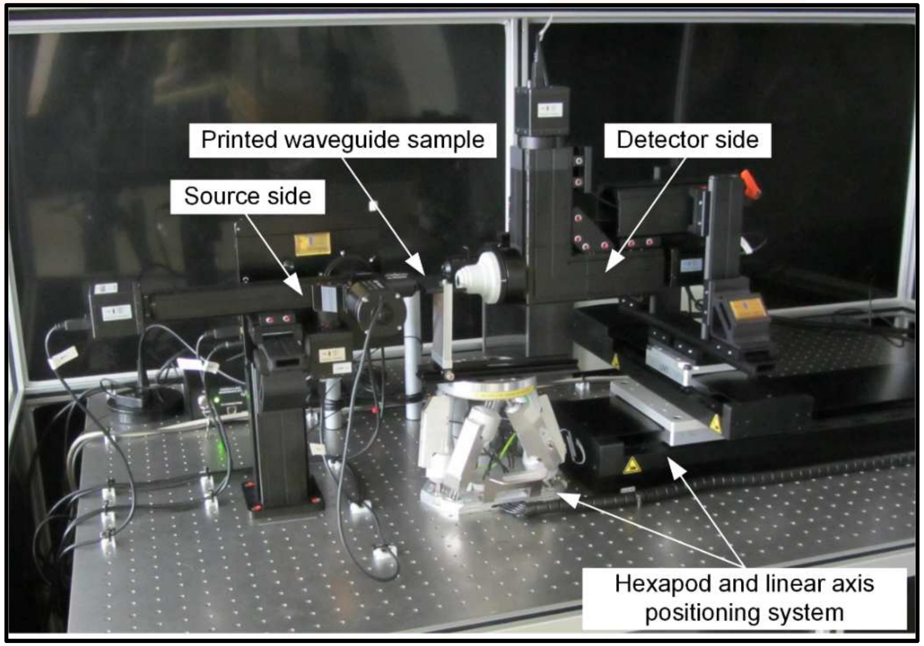

Fig. 51.2: Optical measurement setup (Dumke, ITA, 2014).

Wolfer, Bollgruen, Mager, Overmeyer, Korvink (2014). Flexographic and inkjet printing of polymer optical waveguides for fully integrated sensor systems. Technology Procedia, Elsevier (accepted).

Refractive index measurements

Hot embossing

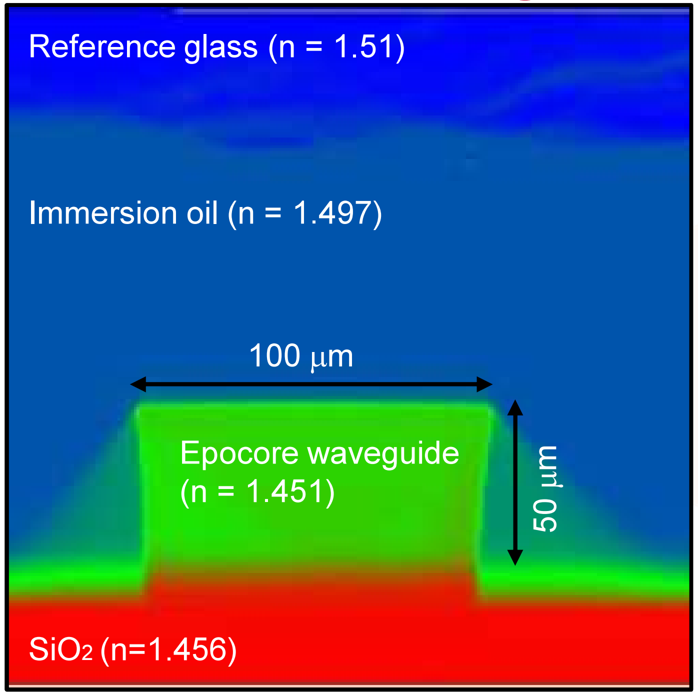

Fig. 53.1: Epocore waveguides structured on a silicon wafer (Günther, 2014).

fs-laser direct writing

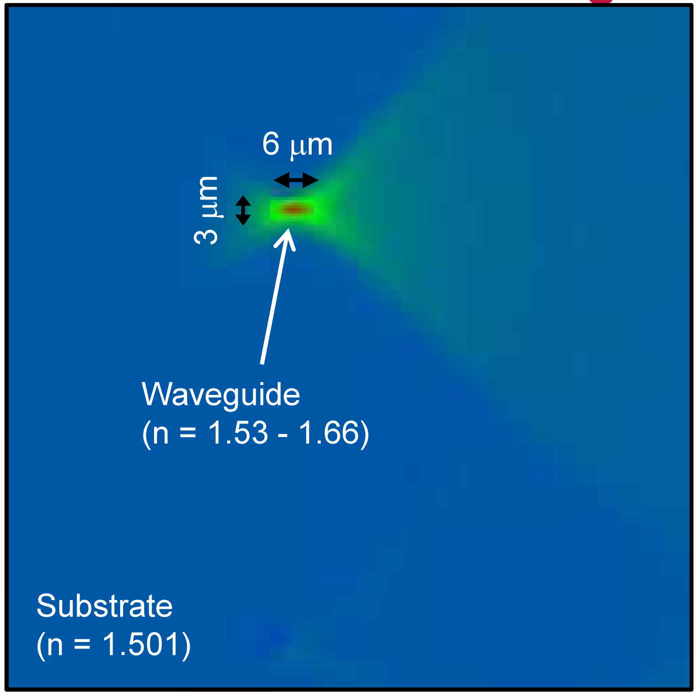

Fig. 53.2: Waveguide written by laser direct writing into the substrate (Günther, 2014).

- Epocore waveguides structured on a silicon wafer
  - ✓ Substrate: silicon
  - ✓ Core material: epocore
  - ✓ Resolution 1.25 µm/pixel

- Profilometer specifications
  - ✓ Refractive index resolution up to 10^{-4}
  - ✓ Spatial resolution: 0.5 µm
  - ✓ Wavelength: 405 nm, 635 nm, 845 nm, 1320 nm

Outline

- Introduction
- Vision of sensor concepts
- Materials
- Production methods
- Characterization
- **Summary**

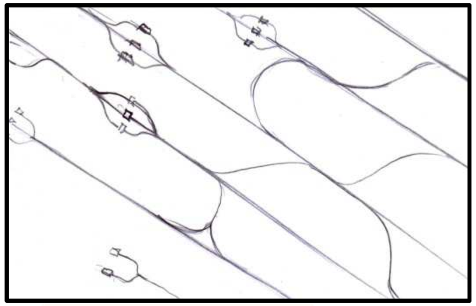

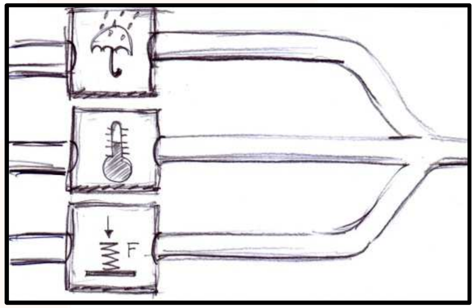

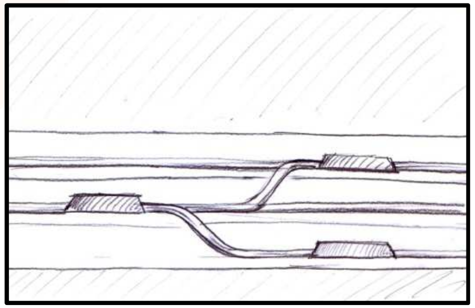

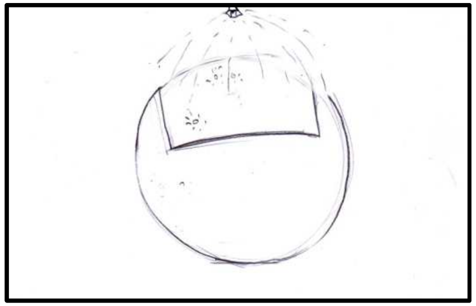

Sensors for excellent flight performances …

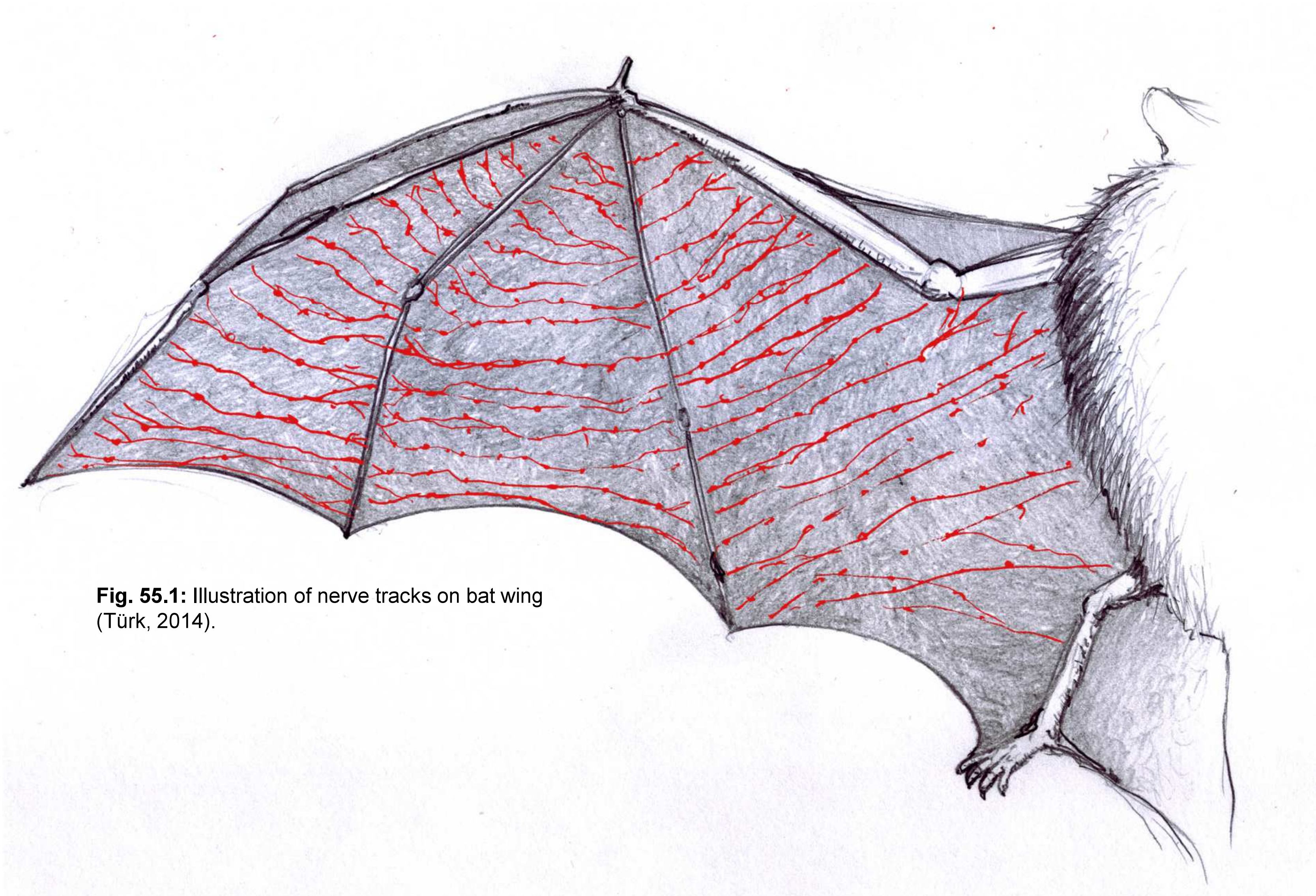

Fig. 55.1: Illustration of nerve tracks on bat wing (Türk, 2014).

… and for stress and temperature surveillance

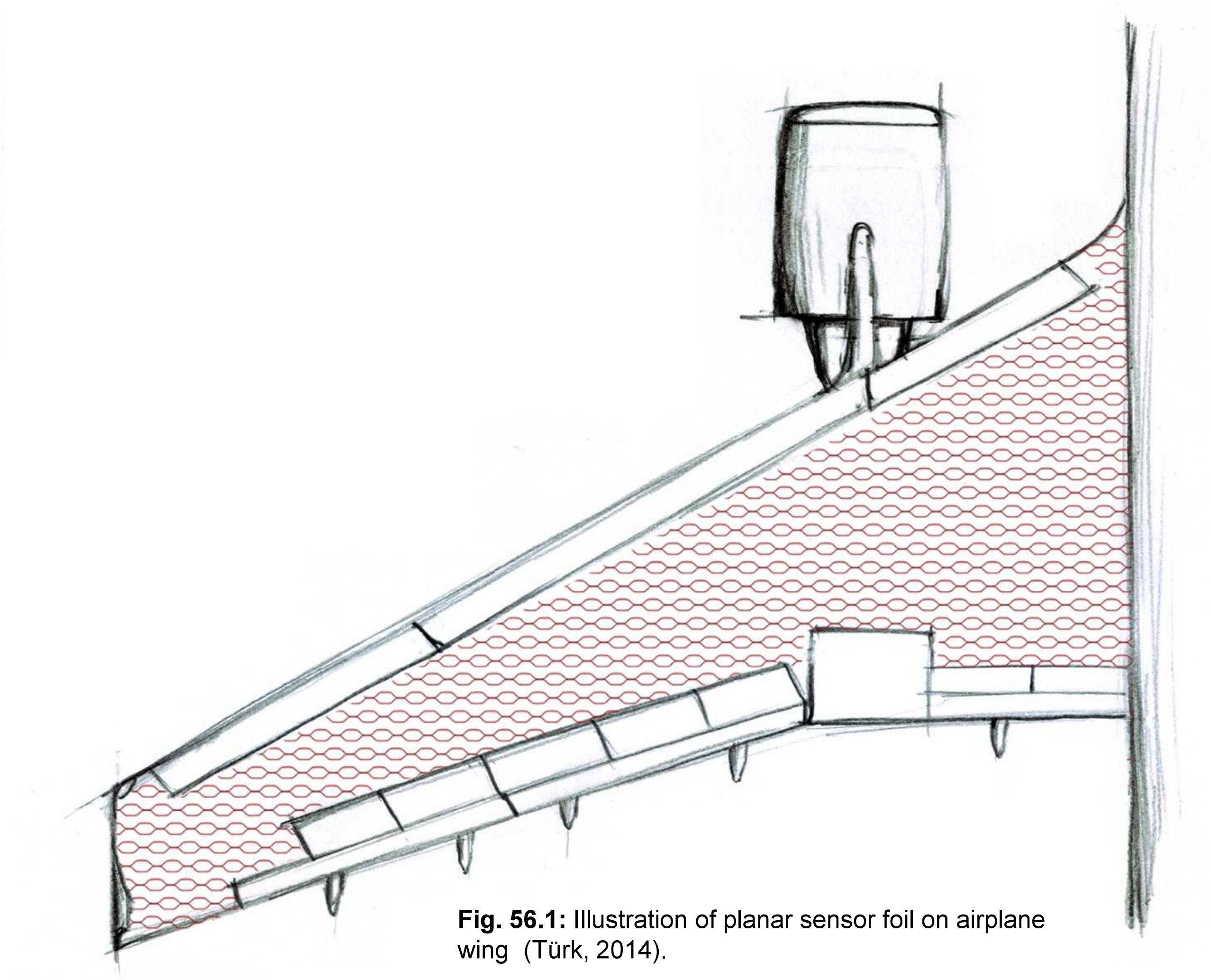

Fig. 56.1: Illustration of planar sensor foil on airplane wing (Türk, 2014).

Summary

- Planar sensors concepts for measurement of
  - ✓ Temperature
  - ✓ Strain
  - ✓ Liquid and gaseous analytes
- Development of thermo-mechanical and chemical stable as well as refractive index tailored polymers
- High throughput production of waveguides in reel-to-reel process - a combination of
  - ✓ Printing
  - ✓ Hot embossing
  - ✓ Laser processing
  - ✓ Lithography
- Optodical bonding as bridging technology
- Equipment available for characterization of
  - ✓ Refractive index
  - ✓ Thickness
  - ✓ Attenuation
  - ✓ Form stability
  - ✓ Glass transition temperature